UNIFORMLY ACCURATE METHODS FOR VLASOV EQUATIONS WITH NON-HOMOGENEOUS STRONG MAGNETIC FIELD

PHILIPPE CHARTIER, NICOLAS CROUSEILLES, MOHAMMED LEMOU, FLORIAN MÉHATS, AND XIAOFEI ZHAO

Abstract. In this paper, we consider *uniformly accurate* methods for solving the highly-oscillatory Vlasov equations with non-homogeneous magnetic field. The specific difficulty (and the resulting novelty of our approach) stems from the presence of a non-periodic oscillation, which necessitates a careful ad-hoc reformulation of the equations by using a confinement property of the solution. A two-scale numerical scheme is proposed where the error estimates show that our scheme not only remains insensitive to the stiffness of the problem in terms of both accuracy and computational cost, but also preserves the confinement property at the discrete level. Our results are illustrated numerically on several examples.

Keywords: Vlasov and Vlasov-Poisson equations, non-homogeneous strong magnetic field, high oscillations, uniform accuracy, two-scale methods.

AMS Subject Classification: 65L05, 65L20, 65L70.

1. Introduction

In this article, we are concerned with the numerical solution of the 2-dimensional Vlasov equation with non-homogeneous magnetic field [2, 4, 16, 17, 25]. More specifically, if $b : x \in \mathbb{R}^2 \mapsto b(x) \in \mathbb{R}$ and $f_0 : (\mathbf{x}, \mathbf{v}) \in \mathbb{R}^2 \times \mathbb{R}^2 \mapsto f_0(\mathbf{x}, \mathbf{v}) \in \mathbb{R}$ are given functions, and if $0 < \varepsilon \leq 1$ denotes a dimensionless parameter and $]0, T]$ a non-empty interval of time, we consider the Cauchy problem for the distribution function $f^\varepsilon : (t, \mathbf{x}, \mathbf{v}) \in [0, T] \times \mathbb{R}^2 \times \mathbb{R}^2 \mapsto f^\varepsilon(t, \mathbf{x}, \mathbf{v}) \in \mathbb{R}$ given by

$$\partial_t f^\varepsilon(t, \mathbf{x}, \mathbf{v}) + \mathbf{v} \cdot \nabla_{\mathbf{x}} f^\varepsilon(t, \mathbf{x}, \mathbf{v}) + \left(\mathbf{E}^\varepsilon(t, \mathbf{x}) + \frac{b(\mathbf{x})}{\varepsilon} J\mathbf{v} \right) \cdot \nabla_{\mathbf{v}} f^\varepsilon(t, \mathbf{x}, \mathbf{v}) = 0, \tag{1.1a}$$

$$f^\varepsilon(0, \mathbf{x}, \mathbf{v}) = f_0(\mathbf{x}, \mathbf{v}), \tag{1.1b}$$

where

(i) the unidirectional magnetic field $B : x \in \mathbb{R}^2 \mapsto B(\mathbf{x}) = (0, 0, b(\mathbf{x})) \in \mathbb{R}^3$ induces a Lorentz force $\mathbf{v} \times B(\mathbf{x})$ which in the two-dimensional context simply becomes $b(\mathbf{x})J\mathbf{v}$ with

$$J = \begin{pmatrix} 0 & 1 \\ -1 & 0 \end{pmatrix}; \tag{1.2}$$

(ii) the electric-field function $\mathbf{E}^\varepsilon : (t, \mathbf{x}) \in \mathbb{R}^+ \times \mathbb{R}^2 \mapsto \mathbf{E}^\varepsilon(t, \mathbf{x}) \in \mathbb{R}^2$ is either external and explicitly given or self-consistent. In the latter case, $\mathbf{E}^\varepsilon$ solves the Poisson equation

$$\nabla_{\mathbf{x}} \cdot \mathbf{E}^\varepsilon(t, \mathbf{x}) = \int_{\mathbb{R}^2} f^\varepsilon(t, \mathbf{x}, \mathbf{v}) d\mathbf{v} - n_i(\mathbf{x}), \tag{1.3}$$

where n_i denotes the ion density of the background.

Solving equation (1.1) with standard methods is notoriously difficult for vanishing values of the parameter ε, as the Lorentz term then creates high-oscillations in the solution: this indeed imposes to use tiny time-steps (usually of the order of ε) and leads to formidable computational costs. Hence, it is now admitted that specific techniques are required that can cope with this particular regime of small values of ε and which, as logic dictates, preserve the asymptotics of f^ε in the limit where ε goes to zero. Numerical methods obeying to this paradigm (i.e. consistent with the limit equation for f^0) and that are consistent with (1.1) when $\varepsilon = O(1)$ have been called *asymptotic preserving* methods and may be found in various publications [18, 19, 20, 22, 24].

Nevertheless, if the value of ε is not known prior to the simulation, it is often observed that the error behaviour of asymptotic-preserving methods is largely deteriorated for certain (not so small) values of ε. As a consequence, it appears highly desirable to design numerical methods for (1.1) which are *uniformly accurate (UA)* with respect to the parameter $\varepsilon \in]0,1]$. That is to say, p^{th}-order methods which, when used with time step Δt, deliver approximate solutions $f^\varepsilon_{\Delta t}$ such that

$$\|f^\varepsilon_{\Delta t} - f^\varepsilon\| \leq C(\Delta t)^p$$

in an appropriate function-norm, where the constant C as well as the computational cost are independent of ε.

It is precisely the aim of this paper to introduce UA schemes for equation (1.1), which, as we shall illustrate numerically, are indeed able to capture the various scales occurring in the system while keeping numerical parameters (in particular the time step) independent of the degree of stiffness ε. Although alternative options are possible [5, 6, 10, 11, 12], the strategy we develop to reach this goal is very much inspired by the recent papers [8, 15]: its main underlying idea consists in separating explicitly the two time scales naturally present in (1.1), namely the slow time t and the fast time t/ε. This is done at the level of the characteristic equations (resulting from the use of the Particle-In-Cell method, see e.g. [1, 27, 23]), which are, for each macro-particles, stiff ordinary differential equations of the form

$$\left\{\begin{array}{rcll} \dot{\mathbf{x}}(t) &=& \mathbf{v}, & \mathbf{x}(0) = \mathbf{x}_0 \\ \dot{\mathbf{v}}(t) &=& \frac{b(\mathbf{x})}{\varepsilon} J\mathbf{v} + \mathbf{E}^\varepsilon(t,\mathbf{x}), & \mathbf{v}(0) = \mathbf{v}_0 \end{array}\right. \tag{1.4}$$

where the term $\frac{b(\mathbf{x})}{\varepsilon} J\mathbf{v}$ is the source of high-oscillations and at the origin of numerical difficulties. As compared to our previous works [8, 10], the main obstacle we are confronted with (and accordingly the main novelty of the proposed solution) is the fact that the aforementioned oscillations are **not per se time-periodic** (see also [7]). However, we will show that the trajectory of the space unknown $\mathbf{x}(t)$ remains confined within an ε-neighbourhood of the initial condition $\mathbf{x}_0$, allowing to regard $e^{\frac{b(\mathbf{x}_0)}{\varepsilon} tJ}$ as the principal oscillation occurring in the solution. *Filtering* it out and *rescaling* the time according to $s = b(\mathbf{x}_0)t$, $\tilde{\mathbf{x}}(s) = \mathbf{x}(t)$, $\tilde{\mathbf{v}}(s) = \mathbf{v}(t)$ and $\tilde{\mathbf{y}}(s) = \mathrm{e}^{-Js/\varepsilon}\tilde{\mathbf{v}}(s)$, we obtain the system

$$\left\{\begin{array}{rcll} \dot{\tilde{\mathbf{x}}}(s) &=& \frac{1}{b(\mathbf{x}_0)} \mathrm{e}^{\frac{s}{\varepsilon}J}\, \tilde{\mathbf{y}}, & \tilde{\mathbf{x}}(0) = \mathbf{x}_0 \\ \dot{\tilde{\mathbf{y}}}(s) &=& \frac{1}{\varepsilon}\left(\frac{b(\tilde{\mathbf{x}})}{b(\mathbf{x}_0)} - 1\right) J\tilde{\mathbf{y}} + \frac{1}{b(\mathbf{x}_0)} \mathrm{e}^{-\frac{s}{\varepsilon}J}\, \mathbf{E}^\varepsilon\left(\frac{s}{b(\mathbf{x}_0)}, \tilde{\mathbf{x}}\right), & \tilde{\mathbf{y}}(0) = \mathbf{v}_0 \end{array}\right. , \tag{1.5}$$

which allows the *embedding* of $\tilde{\mathbf{x}}(s)$ and $\tilde{\mathbf{y}}(s)$ into the functions $X(s,\tau)$ and $Y(s,\tau)$, periodic with respect to τ, and such that $X(s,s/\varepsilon) = \tilde{\mathbf{x}}(s)$ and $Y(s,s/\varepsilon) = \tilde{\mathbf{y}}(s)$. The resulting transport equations

$$\left\{\begin{array}{rcll} \partial_s X + \frac{1}{\varepsilon}\partial_\tau X &=& \frac{1}{b(\mathbf{x}_0)} \mathrm{e}^{\tau J}\, Y, & X(0,0) = \mathbf{x}_0 \\ \partial_s Y + \frac{1}{\varepsilon}\partial_\tau Y &=& \frac{1}{\varepsilon}\left(\frac{b(X)}{b(\mathbf{x}_0)} - 1\right) JY + \frac{1}{b(\mathbf{x}_0)} \mathrm{e}^{-\tau J}\, \mathbf{E}^\varepsilon\left(\frac{s}{b(\mathbf{x}_0)}, X\right), & Y(0,0) = \mathbf{v}_0 \end{array}\right. \tag{1.6}$$

then need to be complemented with initial conditions $X(0,\tau)$ and $Y(0,\tau)$. Their choice is the fundamental ingredient of the two-scale strategy proposed in [8, 13] and it requires to be handled here with additional care owing to the presence of the $1/\varepsilon$-term in the right-hand side of (1.6). Under this form, the problem shares similarities with the model analyzed in [8]. However, (1.6) contains two main additional difficulties due to the presence of the term $(b(X)/b(\mathbf{x}_0) - 1)JY$: first, this nonlinear term prevents a direct application of Gronwall lemma; second, this term is not smooth with respect to the unknown. Finally, we will see that the numerical solution also enjoys a discrete confinement property, i.e. it remains confined within an ε-neighbourhood of the initial data.

The organisation of the paper follows closely the steps exposed above. The two-scale formulation of the characteristics is introduced in Section 2, which includes in particular Subsection 2.1 devoted to the scaling and filtering operations and Subsection 2.3 devoted to the detailed derivation of the initial conditions of (1.6). The section concludes with rigorous estimates of the derivatives of X and Y (see Subsection 2.4) and a numerical confirmation of the expected smoothness of the solution is brought in Subsection 2.5. Section 3 is concerned with the effective derivation of numerical schemes of first and second orders for solving equations (1.6) and the proof of their convergence (Theorem 3.1) which constitutes the main result of this paper. Within Subsection 3.4 the adaptation of our numerical strategy to the situation of a coupling of Vlasov equation with Poisson equation is considered: although no rigorous statement is established at this stage, we provide empirical evidence of the efficiency of our method in this case. Section 4 describes several examples and the corresponding numerical experiments, confirming the interest of the technique.

2. Two-scale formulation of the characteristics equations

In this section, we shall present the strategy to smooth out the fast oscillation on the characteristics of (1.1). Using the Particle-In-Cell (PIC) discretisation,

$$f^\varepsilon(t,\mathbf{x},\mathbf{v}) \approx \sum_{k=1}^{N_p} \omega_k \delta(\mathbf{x}-\mathbf{x}_k(t))\delta(\mathbf{v}-\mathbf{v}_k(t)), \quad t\geq 0,\ \mathbf{x},\mathbf{v}\in\mathbb{R}^2, \tag{2.1}$$

we get the characteristic equation for $1\leq k\leq N_p$,

$$\dot{\mathbf{x}}_k(t) = \mathbf{v}_k(t), \tag{2.2a}$$

$$\dot{\mathbf{v}}_k(t) = \mathbf{E}^\varepsilon(t,\mathbf{x}_k(t)) + \frac{b(\mathbf{x}_k(t))}{\varepsilon}\mathbf{v}_k^\perp(t), \quad t>0, \tag{2.2b}$$

$$\mathbf{x}_k(0) = \mathbf{x}_{k,0}, \quad \mathbf{v}_k(0) = \mathbf{v}_{k,0}. \tag{2.2c}$$

We see (2.2) is a solution-dependent highly oscillatory problem. As a basic requirement throughout the paper, we consider that the magnetic field function $b(\mathbf{x})$ is uniformly above zero, i.e. for some constant $c_0>0$,

$$b(\mathbf{x}) \geq c_0 > 0, \quad \forall \mathbf{x}\in\mathbb{R}^2. \tag{2.3}$$

We shall restrict to consider the Vlasov equation with an external field $\mathbf{E}^\varepsilon$ in this section. In this linear case, particles evolve in an independent way. Hence, we shall remove the particle subscript k in the following of the section for simplicity. We shall show in subsections 2.1-2.2 that through a series of transformations, the highly oscillatory system (2.2) can be formulated into the following two-scale system (see also (2.13)) for $X = X(s,\tau)$, $Y = Y(s,\tau)$

$$\begin{aligned} &\partial_s X + \frac{1}{\varepsilon}\partial_\tau X = \frac{\mathrm{e}^{\tau J}}{b(\mathbf{x}(0))} Y,\\ &\partial_s Y + \frac{1}{\varepsilon}\partial_\tau Y = \frac{1}{\varepsilon}\left(\frac{b(X)}{b(\mathbf{x}(0))}-1\right) JY + \mathrm{e}^{-J\tau}\frac{\mathbf{E}^\varepsilon(s/b(\mathbf{x}(0)),X)}{b(\mathbf{x}(0))}, \quad s>0,\ \tau\in\mathbb{T}, \end{aligned}$$

where $\mathbf{x}(t) = X(b(\mathbf{x}(0))t, b(\mathbf{x}(0))t/\varepsilon)$ and $\mathbf{v}(t) = \mathrm{e}^{Jb(\mathbf{x}(0))t/\varepsilon} Y(b(\mathbf{x}(0))t, b(\mathbf{x}(0))t/\varepsilon)$. With a suitably constructed initial data $X(0,\tau)$, $Y(0,\tau)$ in Section 2.3, we show that the oscillations in the two-scale system in the linear case (i.e. with external given $\mathbf{E}^\varepsilon$) can be smoothed out, i.e. one can make in principle

$$\partial_s^m X(s,\tau), \partial_s^m Y(s,\tau) = O(1), \quad \forall m\in\mathbb{N},\ \varepsilon\in]0,1].$$

The boundedness of these derivative terms is the key-ingredient for the construction of uniformly accurate numerical schemes, as will be proposed in the sequel. For technical reasons, we assume that the given electric field $\mathbf{E}^\varepsilon(t,\mathbf{x})$ and the magnetic field $b(\mathbf{x})$ are globally Lipschitz functions, i.e.

$$\begin{aligned} &|\mathbf{E}^\varepsilon(t,\mathbf{x}_1) - \mathbf{E}^\varepsilon(t,\mathbf{x}_2)| \leq C_{\mathbf{E}}|\mathbf{x}_1-\mathbf{x}_2|, \quad \forall \mathbf{x}_1,\mathbf{x}_2\in\mathbb{R}^2,\ 0\leq t\leq T,\\ &|b(\mathbf{x}_1) - b(\mathbf{x}_2)| \leq C_b|\mathbf{x}_1-\mathbf{x}_2|, \quad \forall \mathbf{x}_1,\mathbf{x}_2\in\mathbb{R}^2, \end{aligned} \tag{2.4}$$

for two constants $C_{\mathbf{E}}, C_b>0$ independent of ε. Here and after, the norm $|\cdot|$ of a vector always refers to the standard euclidian norm in $\mathbb{R}^2$, whereas it refers to the absolute value when it is applied to a scalar quantity. The main result of the section may be stated as follows:

Proposition 2.1. (*i*) *Assume (2.3), (2.4), $E^\varepsilon(t,\mathbf{x})\in\mathcal{C}^2([0,T]\times\mathbb{R}^2)$ and $b(\mathbf{x})\in\mathcal{C}^2(\mathbb{R}^2)$. With the first order initial data $X(0,\tau) = X^{1st}(\tau)$ given by* (2.31) *and $Y(0,\tau)=\mathbf{v}_0$, the solution of the two-scale system (2.13) satisfies*

$$\frac{1}{\varepsilon}\|\partial_s X\|_{L_s^\infty(W_\tau^{1,\infty})} + \|\partial_s Y\|_{L_s^\infty(W_\tau^{1,\infty})} \leq C_0, \tag{2.5}$$

for some constant $C_0>0$ independent of ε.

(ii) Assume (2.3), (2.4), $E^\varepsilon(t,\mathbf{x}) \in \mathcal{C}^3([0,T]\times\mathbb{R}^2)$ and $b(\mathbf{x}) \in \mathcal{C}^3(\mathbb{R}^2)$. With the second order initial data $X(0,\tau) = X^{2nd}(\tau)$ given by (2.38) and $Y(0,\tau) = Y^{1st}(\tau)$ given by (2.34), the solution of the two-scale system (2.13) satisfies

$$\frac{1}{\varepsilon}\|\partial_s^\ell X\|_{L_s^\infty(W_\tau^{1,\infty})} + \|\partial_s^\ell Y\|_{L_s^\infty(W_\tau^{1,\infty})} \leq C_0, \quad \ell = 1,2, \tag{2.6}$$

for some constant $C_0 > 0$ independent of ε.

The proof of the Proposition 2.1 will be given in Section 2.4 and it will be illustrated numerically in Section 2.5.

2.1. **Scaling of time and filtering.** We begin with a transformation on (2.2) with k omitted. For each particle, introduce the scaled time

$$s = b^0\, t, \quad b^0 = b(\mathbf{x}(0)), \tag{2.7}$$

and define

$$\tilde{\mathbf{x}}(s) := \mathbf{x}(t), \quad \tilde{\mathbf{v}}(s) := \mathbf{v}(t), \quad s \geq 0.$$

Note that under the assumption (2.3), $s = s(t)$ is a monotone increasing function, which is interpreted as a time for a particle. Through this transformation, we make each particle living in its own time. Then we can rewrite the characteristics equation (2.2) as

$$\dot{\tilde{\mathbf{x}}}(s) = \frac{\tilde{\mathbf{v}}(s)}{b^0}, \tag{2.8a}$$

$$\dot{\tilde{\mathbf{v}}}(s) = \frac{b(\tilde{\mathbf{x}}(s))}{\varepsilon b^0} J\tilde{\mathbf{v}}(s) + \frac{\mathbf{E}^\varepsilon(s/b^0, \tilde{\mathbf{x}}(s))}{b^0}, \quad s > 0, \tag{2.8b}$$

$$\tilde{\mathbf{x}}(0) = \mathbf{x}_0, \quad \tilde{\mathbf{v}}(0) = \mathbf{v}_0. \tag{2.8c}$$

Next, we isolate the main oscillation term,

$$\dot{\tilde{\mathbf{v}}}(s) = \frac{1}{\varepsilon} J\tilde{\mathbf{v}}(s) + \left(\frac{b(\tilde{\mathbf{x}})}{b^0} - 1\right)\frac{J\tilde{\mathbf{v}}(s)}{\varepsilon} + \frac{\mathbf{E}^\varepsilon(s/b^0, \tilde{\mathbf{x}}(s))}{b^0}, \quad s > 0,$$

and then filter it out by introducing

$$\tilde{\mathbf{y}}(s) := \mathrm{e}^{-Js/\varepsilon}\tilde{\mathbf{v}}(s), \qquad s \geq 0. \tag{2.9}$$

Then (2.8) becomes

$$\dot{\tilde{\mathbf{x}}}(s) = \mathrm{e}^{Js/\varepsilon}\frac{\tilde{\mathbf{y}}(s)}{b^0}, \tag{2.10a}$$

$$\dot{\tilde{\mathbf{y}}}(s) = \left(\frac{b(\tilde{\mathbf{x}}(s))}{b^0} - 1\right)\frac{J\tilde{\mathbf{y}}(s)}{\varepsilon} + \mathrm{e}^{-Js/\varepsilon}\frac{\mathbf{E}^\varepsilon(s/b^0, \tilde{\mathbf{x}}(s))}{b^0}, \quad s > 0, \tag{2.10b}$$

$$\tilde{\mathbf{x}}(0) = \mathbf{x}_0, \quad \tilde{\mathbf{y}}(0) = \mathbf{v}_0. \tag{2.10c}$$

We shall analyse and solve (2.10) up to any fixed time

$$S = Tb^0 > 0.$$

We shall see in the next lemma that the term

$$\left(\frac{b(\tilde{\mathbf{x}}(s))}{b^0} - 1\right)\frac{J\tilde{\mathbf{y}}(s)}{\varepsilon}$$

in (2.10) is actually not stiff, as $\tilde{\mathbf{x}}(s)$ remains close to $\tilde{\mathbf{x}}(0)$ and then $b(\tilde{\mathbf{x}}(s)) - b(\tilde{\mathbf{x}}(0)) = O(\varepsilon)$.

Lemma 2.2. *Under assumption (2.3), (2.4) and $\mathbf{E}^\varepsilon(t,\mathbf{x}) \in C([0,T],\mathbb{R}^2)$, $b(\mathbf{x}) \in \mathcal{C}^1(\mathbb{R}^2)$, for the solution of (2.10), we have that*

$$|\tilde{\mathbf{x}}(s) - \mathbf{x}_0| \leq C_1\varepsilon, \quad |\tilde{\mathbf{y}}(s)| \leq C_2, \quad 0 \leq s \leq S, \tag{2.11}$$

for some $C_1, C_2 > 0$. Hence,

$$\frac{1}{\varepsilon}\left|\frac{b(\tilde{\mathbf{x}}(s))}{b^0} - 1\right| \leq C_3, \quad 0 \leq s \leq S, \tag{2.12}$$

for some $C_3 > 0$. The constants C_1, C_2, C_3 are independent of ε.

Proof. Based on the assumption for $E^\varepsilon(t,\mathbf{x})$ and $b(\mathbf{x})$, we have the global well-posedness of (2.10) and $\tilde{\mathbf{x}}(s),\tilde{\mathbf{y}}(s)\in C(\mathbb{R}^+)$. Indeed, taking the inner product on both sides of (2.10a) and (2.10b) with $\tilde{\mathbf{x}}(s)$ and $\tilde{\mathbf{y}}(s)$ and applying Cauchy-Schwarz inequality gives

$$\frac{d}{ds}|\tilde{\mathbf{x}}(s)|^2 \le \frac{2}{b^0}|\tilde{\mathbf{x}}(s)|\,|\tilde{\mathbf{y}}(s)|,\quad \frac{d}{ds}|\tilde{\mathbf{y}}(s)|^2 \le \frac{2}{b^0}|\mathbf{E}^\varepsilon(s/b^0,\tilde{\mathbf{x}}(s))|\,|\tilde{\mathbf{y}}(s)|.$$

Hence we find

$$\begin{aligned}\frac{d}{ds}|\tilde{\mathbf{x}}(s)| \le& \frac{1}{b^0}|\tilde{\mathbf{y}}(s)|,\\ \frac{d}{ds}|\tilde{\mathbf{y}}(s)| \le& \frac{2}{b^0}|\mathbf{E}^\varepsilon(s/b^0,\tilde{\mathbf{x}}(s))| \le \frac{2}{b^0}\left(|\mathbf{E}^\varepsilon(s/b^0,\mathbf{x}_0)| + C_{\mathbf{E}}|\tilde{\mathbf{x}}(s)-\mathbf{x}_0|\right)\\ \le& \frac{2}{b^0}\|\mathbf{E}^\varepsilon(\cdot,\mathbf{x}_0)\|_{L^\infty(0,T)} + \frac{2C_{\mathbf{E}}}{b^0}|\mathbf{x}_0| + \frac{2C_{\mathbf{E}}}{b^0}|\tilde{\mathbf{x}}(s)|.\end{aligned}$$

Then, adding up the two previous inequalities and using Gronwall's inequality, one can get an *a-priori* bound of the solution

$$|\tilde{\mathbf{x}}(s)| + |\tilde{\mathbf{y}}(s)| \le C_2,\quad 0\le s\le S,$$

where $C_2 = (2/b^0)\left(\|\mathbf{E}^\varepsilon(\cdot,\mathbf{x}_0)\|_{L^\infty(0,T)} + C_{\mathbf{E}}|\mathbf{x}_0|\right)\exp(2T\max\{1,C_{\mathbf{E}}\})$.

By the integral formula of (2.10a) and then integrating by parts, we have

$$\begin{aligned}\tilde{\mathbf{x}}(s) &= \tilde{\mathbf{x}}(0) + \int_0^s \mathrm{e}^{J\theta/\varepsilon}\frac{\tilde{\mathbf{y}}(\theta)}{b^0}d\theta\\ &= \tilde{\mathbf{x}}(0) - \frac{J\varepsilon}{b^0}\left(\mathrm{e}^{Js/\varepsilon}\tilde{\mathbf{y}}(s) - \tilde{\mathbf{y}}(0)\right) + \varepsilon J\int_0^s \mathrm{e}^{J\theta/\varepsilon}\frac{\dot{\tilde{\mathbf{y}}}(\theta)}{b^0}d\theta.\end{aligned}$$

Hence from (2.10b), we have

$$\begin{aligned}\tilde{\mathbf{x}}(s) =& \tilde{\mathbf{x}}(0) - \frac{J\varepsilon}{b^0}\left(\mathrm{e}^{Js/\varepsilon}\tilde{\mathbf{y}}(s) - \tilde{\mathbf{y}}(0)\right)\\ &+ \varepsilon J\int_0^s \frac{\mathrm{e}^{J\theta/\varepsilon}}{b^0}\left[\left(\frac{b(\tilde{\mathbf{x}}(\theta))}{b^0}-1\right)\frac{J\tilde{\mathbf{y}}(\theta)}{\varepsilon} + \mathrm{e}^{-J\theta/\varepsilon}\frac{\mathbf{E}^\varepsilon(\theta/b^0,\tilde{\mathbf{x}}(\theta))}{b^0}\right]d\theta.\end{aligned}$$

Then we can see for all $0\le s\le S$,

$$\frac{1}{\varepsilon}\left|\tilde{\mathbf{x}}(s)-\mathbf{x}_0\right| \le \frac{1}{b^0}\left(C_2 + |\mathbf{y}_0|\right) + T\|\mathbf{E}^\varepsilon\|_\infty + \frac{C_2C_b}{(b^0)^2}\int_0^s \frac{1}{\varepsilon}\left|\tilde{\mathbf{x}}(\theta)-\mathbf{x}_0\right|d\theta,$$

where

$$\|\mathbf{E}^\varepsilon\|_\infty := \sup\{|\mathbf{E}^\varepsilon(t,\mathbf{x})| : 0\le t\le T,\, |\mathbf{x}|\le C_2\}.$$

By Gronwall's inequality, we get estimate

$$\frac{1}{\varepsilon}\left|\tilde{\mathbf{x}}(s)-\mathbf{x}_0\right| \le C_1,\quad \forall 0\le s\le S,$$

for a constant $C_1>0$ independent of ε. Inequality (2.12) then follows from

$$b(\tilde{\mathbf{x}}(s)) - b^0 = \int_0^s \nabla_{\mathbf{x}} b\left(\theta\tilde{\mathbf{x}}(s) + (1-\theta)\tilde{\mathbf{x}}(0)\right)d\theta\cdot(\tilde{\mathbf{x}}(s)-\tilde{\mathbf{x}}(0)).$$

□

Thanks to Lemma 2.2, we observe that the right-hand-side of (2.10) is bounded as $\varepsilon\to 0$. If we consider that $\mathbf{E}^\varepsilon(t,\mathbf{x})$ is a given external field and contains no fast frequency in the t-variable, the formulation (2.10) fits the requirement of the two-scale strategy.

2.2. **Two-scale formulation.** As stated in beginning of this section, we consider first of all the case that $\mathbf{E}^\varepsilon(t,\mathbf{x})$ is a given external field without any fast frequencies in the t-variable. We shall address the Vlasov-Poisson case later. We are going to derive the two-scale model from (2.10) by assuming t and t/ε are independent, like in [15] and this two-scale model will be the model for numerical discretisation in the next section.

Now we perform the two-scale formulation on (2.10). Denote the fast variable $\tau = s/\varepsilon$ and separate it out in (2.10), then we have

$$\partial_s X + \frac{1}{\varepsilon}\partial_\tau X = \frac{\mathrm{e}^{\tau J}}{b^0}Y, \tag{2.13a}$$

$$\partial_s Y + \frac{1}{\varepsilon}\partial_\tau Y = \frac{1}{\varepsilon}\left(\frac{b(X)}{b^0} - 1\right)JY + \mathrm{e}^{-J\tau}\frac{\mathbf{E}^\varepsilon(s/b^0, X)}{b^0}, \quad s > 0,\ \tau \in \mathbb{T}, \tag{2.13b}$$

where $X = X(s,\tau)$, $Y = Y(s,\tau)$ and $\mathbb{T} = \mathbb{R}/(2\pi)$ is a torus. Choosing $X(0,0) = \mathbf{x}(0)$, $Y(0,0) = \mathbf{v}(0)$, we recover the original unknown by considering the two-scale unknown on the diagonal $\tau = s/\varepsilon$

$$X(s, s/\varepsilon) = \tilde{\mathbf{x}}(s), \quad Y(s, s/\varepsilon) = \tilde{\mathbf{y}}(s), \quad s \geq 0. \tag{2.14}$$

In the next section, numerical schemes will be proposed for the two-scale system (2.13), and our aim will be to prove that these schemes enjoy uniform accuracy with respect to ε. This property requires a preliminary analysis. Indeed, one can observe that no initial condition for (2.13) is evident since only the condition $X(0,0) = \mathbf{x}(0)$, $Y(0,0) = \mathbf{v}(0)$ is required. This degree of freedom will be used to derive initial conditions $X(0,\tau)$, $Y(0,\tau)$ such that the two-scale unknown $X(s,\tau)$, $Y(s,\tau)$ and its time derivative are uniformly bounded. This will be the objective of the rest of this section.

First, we start with the following elementary lemma

Lemma 2.3. *Let $\mathcal{H}$ be a Banach algebra space of real-valued functions and let $\mathcal{H}^2$ denote the cartesian product $\mathcal{H}\times\mathcal{H}$. Consider the following system of ordinary differential equations in $\mathcal{H}^2$ (i.e. X^ε and Y^ε are considered as functions from $[0,S]$ to $\mathcal{H}^2$)*

$$\begin{aligned} \frac{dX^\varepsilon}{ds} &= \frac{1}{\varepsilon}e^{Js/\varepsilon}Y^\varepsilon, \\ \frac{dY^\varepsilon}{ds} &= \alpha^\varepsilon(s)Y^\varepsilon + \beta^\varepsilon(s)X^\varepsilon + \gamma^\varepsilon(s), \\ X^\varepsilon(0) = X_0, &\qquad Y^\varepsilon(0) = Y_0 \quad \textit{two given initial data,} \end{aligned}$$

with $\alpha^\varepsilon(s), \beta^\varepsilon(s)$ are 2×2 matrices with coefficients in $\mathcal{H}$ and $\gamma^\varepsilon : [0,S] \to \mathcal{H}^2$. Assume that there exists a constant $C > 0$ independent of ε such that $\|\alpha^\varepsilon(s)\|_{\mathcal{H}} \leq C$, $\|\beta^\varepsilon(s)\|_{\mathcal{H}} \leq C$ and $\|\gamma^\varepsilon(s)\|_{\mathcal{H}} \leq C$, $\forall s \in [0,S]$. Then there exists a constant $M > 0$ independent of ε such that

$$\|X^\varepsilon(s)\|_{\mathcal{H}^2} + \|Y^\varepsilon(s)\|_{\mathcal{H}^2} \leq M(1 + \|X_0\|_{\mathcal{H}^2} + \|Y_0\|_{\mathcal{H}^2}),\ \forall s \in [0,S].$$

Proof. We integrate the equation on X^ε and perform an integration by parts to get

$$\begin{aligned} X^\varepsilon(s) &= X_0 + \frac{1}{\varepsilon}\int_0^s e^{J\sigma/\varepsilon}Y^\varepsilon(\sigma)d\sigma \\ &= X_0 + \frac{1}{\varepsilon}\left\{\left[-\varepsilon J e^{J\sigma/\varepsilon}Y^\varepsilon(\sigma)\right]_0^s + \varepsilon J\int_0^s e^{J\sigma/\varepsilon}\frac{dY^\varepsilon(\sigma)}{ds}d\sigma\right\} \\ &= X_0 - Je^{Js/\varepsilon}Y^\varepsilon(s) + JY_0 + \varepsilon J\int_0^s e^{J\sigma/\varepsilon}\left[\alpha^\varepsilon(\sigma)Y^\varepsilon(\sigma) + \beta^\varepsilon(\sigma)X^\varepsilon(\sigma) + \gamma^\varepsilon(\sigma)\right]d\sigma, \end{aligned}$$

where we used the equation on Y^ε. We always use C in proofs to denote a positive constant independent of ε, and its value may change from one line to the next. Considering the norm $\|\cdot\|_{\mathcal{H}}^2$ leads to

$$\|X^\varepsilon(s)\|_{\mathcal{H}^2} \leq \|X_0\|_{\mathcal{H}^2} + C\|Y_0\|_{\mathcal{H}^2} + \|Y^\varepsilon(s)\|_{\mathcal{H}^2} + C + C\int_0^s \left[\|Y^\varepsilon(\sigma)\|_{\mathcal{H}^2} + \|X^\varepsilon(\sigma)\|_{\mathcal{H}^2}\right]d\sigma,$$

using $\|e^{J\tau}u\|_{\mathcal{H}^2} \le \|u\|_{\mathcal{H}^2}$ for all $u \in \mathcal{H}^2$, with C independent of τ. Integrating now the equation on Y^ε gives directly

$$\|Y^\varepsilon(s)\|_{\mathcal{H}^2} \le \|Y_0\|_{\mathcal{H}^2} + C + C\int_0^s [\|Y^\varepsilon(\sigma)\|_{\mathcal{H}^2} + \|X^\varepsilon(\sigma)\|_{\mathcal{H}^2}]\,d\sigma,$$

which reported in the former inequality gives

$$\|X^\varepsilon(s)\|_{\mathcal{H}^2} \le C(\|X_0\|_{\mathcal{H}^2} + \|Y_0\|_{\mathcal{H}^2}) + C + C\int_0^s [\|Y^\varepsilon(\sigma)\|_{\mathcal{H}^2} + \|X^\varepsilon(\sigma)\|_{\mathcal{H}^2}]\,d\sigma.$$

The two last inequalities clearly lead to

$$\|X^\varepsilon(s)\|_{\mathcal{H}^2} + \|Y^\varepsilon(s)\|_{\mathcal{H}^2} \le C(\|X_0\|_{\mathcal{H}^2} + \|Y_0\|_{\mathcal{H}^2}) + C + C\int_0^s [\|Y^\varepsilon(\sigma)\|_{\mathcal{H}^2} + \|X^\varepsilon(\sigma)\|_{\mathcal{H}^2}]\,d\sigma.$$

A standard Gronwall lemma enables to prove the result of the lemma. □

For convenience, we shall denote $L^\infty_s := L^\infty_s([0,S])$ and $L^\infty_\tau := L^\infty_\tau(\mathbb{T})$ the functional spaces in s and τ variables. Now, for a smooth periodic function $u(\tau)$ on $\mathbb{T}$, we introduce

$$\|u\|_{W^{1,\infty}_\tau} = \max\left\{\|u\|_{L^\infty_\tau}, \|\partial_\tau u\|_{L^\infty_\tau}\right\}.$$

For a smooth vector field $\mathbf{U}(\tau)$ on $\mathbb{T}$, we define its $W^{1,\infty}_\tau$-norm as

$$\|\mathbf{U}\|_{W^{1,\infty}_\tau} = \max\left\{\|u_1\|_{W^{1,\infty}_\tau}, \|u_2\|_{W^{1,\infty}_\tau}\right\}, \quad \text{for} \quad \mathbf{U}(\tau) = \begin{pmatrix} u_1(\tau) \\ u_2(\tau)\end{pmatrix}.$$

The following lemma shows that in the two-scale system (2.13), the term

$$\frac{1}{\varepsilon}\left(\frac{b(X)}{b^0} - 1\right) JY$$

is not stiff when $\varepsilon \to 0$.

Lemma 2.4. *Assume (2.3), (2.4) and $E^\varepsilon(t,\mathbf{x}) \in \mathcal{C}^1([0,T]\times\mathbb{R}^2)$ and $b(\mathbf{x}) \in \mathcal{C}^1(\mathbb{R}^2)$. For the two-scale problem (2.13), if initially*

$$\frac{1}{\varepsilon}\|X(0,\cdot) - \mathbf{x}_0\|_{W^{1,\infty}_\tau} + \|Y(0,\cdot)\|_{W^{1,\infty}_\tau} \le C_0, \tag{2.15}$$

for some constant $C_0 > 0$ independent of ε, then

$$\frac{1}{\varepsilon}\|X - \mathbf{x}_0\|_{L^\infty_s(W^{1,\infty}_\tau)} + \|Y\|_{L^\infty_s(W^{1,\infty}_\tau)} \le C_1, \tag{2.16}$$

for some $C_1 > 0$ independent of ε. Hence,

$$\frac{1}{\varepsilon}\left\|\frac{b(X)}{b^0} - 1\right\|_{L^\infty_s(W^{1,\infty}_\tau)} \le C_2, \tag{2.17}$$

for some $C_2 > 0$ independent of ε.

Proof. Consider τ as a parameter in $\mathbb{T}$ and define

$$X_\tau(s) := X\left(s, \tau + \frac{s}{\varepsilon}\right), \quad Y_\tau(s) := Y\left(s, \tau + \frac{s}{\varepsilon}\right), \quad s \ge 0. \tag{2.18}$$

The two scale problem (2.13) then reads

$$\dot{X}_\tau = \frac{\mathrm{e}^{J(\tau+s/\varepsilon)}}{b^0}Y_\tau, \tag{2.19a}$$

$$\dot{Y}_\tau = \frac{1}{\varepsilon}\left(\frac{b(X_\tau)}{b^0} - 1\right) JY_\tau + \mathrm{e}^{-J(\tau+s/\varepsilon)}\frac{\mathbf{E}^\varepsilon(s/b^0, X_\tau)}{b^0}, \quad s > 0. \tag{2.19b}$$

Using the same strategy as in the proof of Lemma 2.2, we have

$$|X(s,\tau+s/\varepsilon) - \mathbf{x}_0| \le C\varepsilon \text{ and } |Y(s,\tau+s/\varepsilon)| \le C, \ \ \forall\, 0 \le s \le S,\ 0 \le \tau \le 2\pi,$$

so that

$$\|X(s,\cdot) - \mathbf{x}_0\|_{L^\infty_\tau} \le C\varepsilon, \quad 0 \le s \le S. \tag{2.20}$$

From now, we focus on the τ-derivative to get $W^{1,\infty}_\tau$ estimate. First, we rewrite (2.19) by considering the new unknown $\tilde{Y}_\tau = \frac{e^{\tau J}}{b^0} Y_\tau$

$$\dot{X}_\tau = e^{Js/\varepsilon}\tilde{Y}_\tau, \tag{2.21a}$$

$$\dot{\tilde{Y}}_\tau = \frac{1}{\varepsilon}\left(\frac{b(X_\tau)}{b^0} - 1\right) J\tilde{Y}_\tau + e^{-Js/\varepsilon}\frac{\mathbf{E}^\varepsilon(s/b^0, X_\tau)}{(b^0)^2}, \quad s > 0. \tag{2.21b}$$

Taking now the derivative with respect to τ of (2.21) and denoting

$$\hat{X}_\tau(s,\tau) := \frac{1}{\varepsilon}\partial_\tau X_\tau(s,\tau), \quad \hat{Y}_\tau(s,\tau) := \partial_\tau \tilde{Y}_\tau(s,\tau) \tag{2.22}$$

we get

$$\dot{\hat{X}}_\tau = \frac{e^{Js/\varepsilon}}{\varepsilon}\hat{Y}_\tau, \tag{2.23a}$$

$$\dot{\hat{Y}}_\tau = \frac{1}{\varepsilon}\left(\frac{b(X_\tau)}{b^0} - 1\right) J\hat{Y}_\tau + \nabla_{\mathbf{x}} b(X_\tau)\cdot \hat{X}_\tau J\tilde{Y}_\tau + \varepsilon\frac{e^{-Js/\varepsilon}}{(b^0)^2}\nabla_{\mathbf{x}}\mathbf{E}^\varepsilon(s/b^0, X_\tau)\hat{X}_\tau \tag{2.23b}$$

Now, using Lemma 2.3 with $\mathcal{H} = L^\infty_\tau([0, 2\pi])$ and (2.20), we conclude that

$$\|\hat{X}_\tau(s,\cdot)\|_{L^\infty_\tau} + \|\hat{Y}_\tau(s,\cdot)\|_{L^\infty_\tau} \le C, \ \ \forall 0 \le s \le S,$$

since $\hat{X}_\tau(0,\cdot) = O(1)$ and $\hat{Y}_\tau(0,\cdot) = O(1)$ by assumption, which concludes the proof. □

2.3. **Suitable initial data for the two-scale formulation.** In this subsection, we look for an initial data $X(0,\tau), Y(0,\tau)$ of the two-scale formulation (2.13), which will ensure that the time derivatives of the solutions $X(s,\tau), Y(s,\tau)$ are uniformly bounded. This will be done using Chapman-Enskog expansion of the solution.

First order preparation. We perform the Chapman-Enskog expansion to get the full initial data $X(0,\tau)$, $Y(0,\tau)$ for (2.13). This will be done by formal arguments and a rigorous statement will be proved in the next subsection.

Denote

$$X(s,\tau) = \underline{X}(s) + \mathbf{h}(s,\tau), \quad Y(s,\tau) = \underline{Y}(s) + \mathbf{r}(s,\tau), \tag{2.24}$$

where

$$\underline{X}(s) = \Pi X(s,\tau), \quad \underline{Y}(s) = \Pi Y(s,\tau),$$

with the average operator Π defined for some periodic function $u(\tau)$ on $\mathbb{T}$ as $\Pi u = \frac{1}{2\pi}\int_0^{2\pi} u(\theta)d\theta$. Denoting $Lu(\tau) = \partial_\tau u(\tau)$, we have

$$\begin{cases} \partial_s \underline{X} = \Pi e^{\tau J}\dfrac{Y}{b^0}, \quad s > 0, \ \tau \in \mathbb{T}, \\ \partial_s \mathbf{h} + \dfrac{1}{\varepsilon} L\mathbf{h} = (I - \Pi) e^{\tau J}\dfrac{Y}{b^0}, \end{cases} \tag{2.25}$$

and

$$\begin{cases} \partial_s \underline{Y} = \Pi\left[\dfrac{1}{\varepsilon}\left(\dfrac{b(X)}{b^0} - 1\right) JY + e^{-J\tau}\dfrac{\mathbf{E}^\varepsilon(s/b^0, X)}{b^0}\right], \quad s > 0, \ \tau \in \mathbb{T}, \\ \partial_s \mathbf{r} + \dfrac{1}{\varepsilon} L\mathbf{r} = (I - \Pi)\left[\dfrac{1}{\varepsilon}\left(\dfrac{b(X)}{b^0} - 1\right) JY + e^{-J\tau}\dfrac{\mathbf{E}^\varepsilon(s/b^0, X)}{b^0}\right]. \end{cases} \tag{2.26}$$

Taking the inverse of L, which for a zero average function $u(\tau)$ is computed as $L^{-1}u(\tau) = (I - \Pi)\int_0^\tau u(\theta)d\theta$, on the above equations for $\mathbf{h}$ and $\mathbf{r}$ and denoting $A := L^{-1}(I - \Pi)$, we get

$$\mathbf{h}(s,\tau) = \varepsilon A e^{\tau J}\frac{Y}{b^0} - \varepsilon L^{-1}\partial_s \mathbf{h}, \tag{2.27a}$$

$$\mathbf{r}(s,\tau) = A\left(\frac{b(X)}{b^0} - 1\right) JY + \varepsilon A e^{-J\tau}\frac{\mathbf{E}^\varepsilon(s/b^0, X)}{b^0} - \varepsilon L^{-1}\partial_s \mathbf{r}. \tag{2.27b}$$

Assuming that $\partial_s \mathbf{h}, \partial_s \mathbf{r} = O(1)$ as $\varepsilon \to 0$, from (2.27a) we have firstly

$$\mathbf{h}(s,\tau) = O(\varepsilon), \quad s \ge 0, \ \tau \in \mathbb{T}.$$

Thanks to Lemma 2.4, we have $b(X)/b^0 - 1 = O(\varepsilon)$, and consequently from (2.27b) we get

$$\mathbf{r}(s,\tau) = O(\varepsilon), \quad s \geq 0,\ \tau \in \mathbb{T}.$$

We now take the time derivative of (2.27)

$$\partial_s \mathbf{h}(s,\tau) = \frac{\varepsilon}{b^0} A \mathrm{e}^{\tau J} \left(\partial_s \underline{Y} + \partial_s \mathbf{r}\right) - \varepsilon L^{-1} \partial_s^2 \mathbf{h}, \tag{2.28a}$$

$$\begin{aligned}\partial_s \mathbf{r}(s,\tau) = {} & A\left(\frac{b(X)}{b^0} - 1\right) J \left(\partial_s \underline{Y} + \partial_s \mathbf{r}\right) + \frac{1}{b^0} A \nabla_{\mathbf{x}} b(X) \cdot (\partial_s \underline{X} + \partial_s \mathbf{h}) J Y \\ & + \frac{\varepsilon}{b^0} A \mathrm{e}^{-J\tau} \left(\frac{\partial_t \mathbf{E}^\varepsilon(s/b^0, X)}{b^0} + \nabla_{\mathbf{x}} \mathbf{E}^\varepsilon(s/b^0, X)(\partial_s \underline{X} + \partial_s \mathbf{h})\right) - \varepsilon L^{-1} \partial_s^2 \mathbf{r}. \end{aligned} \tag{2.28b}$$

Assuming that $\partial_s^2 \mathbf{h}, \partial_s^2 \mathbf{r} = O(1)$ and observing that $\partial_s \underline{X} = \Pi(\mathrm{e}^{\tau J} \mathbf{r})/b^0 = O(\varepsilon)$, we get $\partial_s \mathbf{h}, \partial_s \mathbf{r} = O(\varepsilon)$.

We then obtain the first order asymptotic expansions from (2.27)

$$\begin{aligned}\mathbf{h}(0,\tau) = {} & \frac{\varepsilon}{b^0} A \mathrm{e}^{\tau J} \underline{Y}(0) + O(\varepsilon^2), \\ \mathbf{r}(0,\tau) = {} & A\left(\frac{b\left(\underline{X}(0) + \mathbf{h}(0,\tau)\right)}{b^0} - 1\right) J \underline{Y}(0) \quad + \varepsilon A \mathrm{e}^{-J\tau} \frac{\mathbf{E}^\varepsilon(0, \underline{X}(0))}{b^0} + O(\varepsilon^2),\end{aligned}$$

To determine $\mathbf{h}$ and $\mathbf{r}$ at $s = 0$, we then need to compute $\underline{X}(0)$ and $\underline{Y}(0)$. These quantities will be determined from the initial conditions $\mathbf{x}_0$ and $\mathbf{v}_0$. Indeed, we recall that

$$\mathbf{x}_0 = \underline{X}(0) + \mathbf{h}(0,0), \qquad \mathbf{v}_0 = \underline{Y}(0) + \mathbf{r}(0,0). \tag{2.29}$$

Since $\mathbf{h} = O(\varepsilon)$, we have

$$\mathbf{h}(0,\tau) = \mathbf{h}^{1st}(\tau) + O(\varepsilon^2), \text{ with } \mathbf{h}^{1st}(\tau) := \frac{\varepsilon}{b^0} A \mathrm{e}^{\tau J} \mathbf{v}_0 = -\frac{\varepsilon}{b^0} J \mathbf{e}^{\tau J} \mathbf{v}_0,$$

so that we get the following first order expansion for X

$$X(0,\tau) = \underline{X}(0) + \mathbf{h}^{1st}(\tau) + O(\varepsilon^2),$$

and

$$X(0,\tau) = X^{1st}(\tau) + O(\varepsilon^2), \tag{2.30}$$

where, using (2.29) we define

$$\begin{aligned} X^{1st}(\tau) & := \mathbf{x}_0 + \mathbf{h}^{1st}(\tau) - \mathbf{h}^{1st}(0) \\ & = \mathbf{x}_0 - \frac{\varepsilon}{b^0} J(\mathbf{e}^{\tau J} - I)\mathbf{v}_0. \end{aligned} \tag{2.31}$$

Note that owing to $\mathbf{r} = O(\varepsilon)$, we have

$$\mathbf{r}(0,\tau) = A\left(\frac{b\left(X^{1st}(\tau)\right)}{b^0} - 1\right) J \mathbf{v}_0 + \varepsilon A \mathrm{e}^{-J\tau} \frac{\mathbf{E}^\varepsilon(0, \mathbf{x}_0)}{b^0} + O(\varepsilon^2).$$

We then derive a first order expansion for Y

$$Y(0,\tau) = \underline{Y}(0) + \mathbf{r}^{1st}(\tau) + O(\varepsilon^2),$$

with

$$\mathbf{r}^{1st}(\tau) := A\left(\frac{b(X^{1st}(\tau))}{b^0} - 1\right) J \mathbf{v}_0 + \varepsilon J \mathbf{e}^{-\tau J} \frac{\mathbf{E}^\varepsilon(0, \mathbf{x}_0)}{b^0}. \tag{2.32}$$

We combine this identity with (2.29) to get the first order approximation of Y

$$Y(0,\tau) = Y^{1st}(\tau) + O(\varepsilon^2), \tag{2.33}$$

where

$$\begin{aligned} Y^{1st}(\tau) & := \mathbf{v}_0 + \mathbf{r}^{1st}(\tau) - \mathbf{r}^{1st}(0), \\ & = \mathbf{v}_0 + \int_0^\tau (I - \Pi)\left[\frac{b(X^{1st}(\sigma))}{b^0} - 1\right] d\sigma J \mathbf{v}_0 + \varepsilon J(\mathbf{e}^{-\tau J} - I)\frac{\mathbf{E}^\varepsilon(0, \mathbf{x}_0)}{b^0}. \end{aligned} \tag{2.34}$$

Second order preparation. We continue the preparation of initial data to the second order in ε. Inserting (2.28a) in (2.27a) and using $\partial_s \mathbf{r} = O(\varepsilon)$ and $Y(0,\tau) - Y^{1st}(\tau) = O(\varepsilon^2)$, we get

$$\mathbf{h}(0,\tau) \quad = \quad \varepsilon A \mathrm{e}^{\tau J} \frac{Y^{1st}(\tau)}{b^0} - \frac{\varepsilon^2}{b^0} L^{-1} A \mathrm{e}^{\tau J} \partial_s \underline{Y}(0) + O(\varepsilon^3), \tag{2.35}$$

where we assumed $\partial_s^3 \mathbf{h} = O(1)$ which implies as above that $\partial_s^2 \mathbf{h} = O(\varepsilon)$. Now, from (2.26), since $X(s,\tau) - \underline{X}(s) = O(\varepsilon)$ and $X(0,\tau) - X^{1st}(\tau) = O(\varepsilon^2)$, we can write

$$\begin{aligned} \partial_s \underline{Y}(0) \quad &= \quad \Pi \left[\frac{1}{\varepsilon} \left(\frac{b(X^{1st})}{b^0} - 1 \right) J \underline{Y}(0) + \mathrm{e}^{-J\tau} \frac{\mathbf{E}^\varepsilon(0, \underline{X}(0))}{b^0} \right] + O(\varepsilon) \\ &= \quad \Pi \left[\frac{1}{\varepsilon} \left(\frac{b(X^{1st})}{b^0} - 1 \right) \right] J \underline{Y}(0) + O(\varepsilon), \end{aligned}$$

using $\Pi \mathrm{e}^{-\tau J} = 0$. We then define $\mathbf{h}^{2nd}(\tau)$ ($\mathbf{h} = \mathbf{h}^{2nd} + O(\varepsilon^3)$) by injecting the previous expansion in (2.35) to get

$$\mathbf{h}^{2nd}(\tau) := \frac{\varepsilon}{b^0} A(\mathrm{e}^{\tau J} Y^{1st}) - \frac{\varepsilon^2}{b^0} L^{-1} A \mathrm{e}^{\tau J} \Pi \left[\frac{1}{\varepsilon} \left(\frac{b(X^{1st})}{b^0} - 1 \right) \right] J \mathbf{v}_0, \tag{2.36}$$

since $\underline{Y}(0) = \mathbf{v}_0 + O(\varepsilon)$ by (2.29). We then get the following second order expansion for X

$$X(0,\tau) = \underline{X}(0) + \mathbf{h}^{2nd}(\tau) + O(\varepsilon^3),$$

so that

$$X(0,\tau) = X^{2nd}(\tau) + O(\varepsilon^3), \tag{2.37}$$

where, using (2.29) we define

$$X^{2nd}(\tau) := \mathbf{x}_0 + \mathbf{h}^{2nd}(\tau) - \mathbf{h}^{2nd}(0), \tag{2.38}$$

where $\mathbf{h}^{2nd}$ is given by (2.36) and where X^{1st}, Y^{1st} are given by (2.31) and (2.34).

Let us deal with the second order expansion of Y. From (2.27b), we get

$$\mathbf{r}(0,\tau) := A\, B(X^{2nd}) J Y^{1st} + \frac{\varepsilon}{b^0} A \mathrm{e}^{-J\tau} \mathbf{E}^\varepsilon(0, X^{1st}) - \varepsilon L^{-1} \partial_s \mathbf{r} + O(\varepsilon^3), \tag{2.39}$$

with $B(X) = \frac{b(X)}{b^0} - 1$. Therefore, it remains to find an expansion of $\partial_s \mathbf{r}$ (given by (2.28b)) up to order 1 in ε. To that purpose, we use (2.28b), (2.28a) and the first equation of (2.26). We find $\partial_s \mathbf{r}(0,\tau) = \mathcal{T}^{2nd}(\tau) + O(\varepsilon^2)$ where $\mathcal{T}^{2nd}$ is given by

$$\begin{aligned} \mathcal{T}^{2nd}(\tau) = {} & \frac{1}{\varepsilon} A B(X^{1st}) J \Pi \left[B(X^{1st}) J \mathbf{v}_0 \right] + \frac{\varepsilon}{(b^0)^2} A \mathrm{e}^{-\tau J} \partial_t \mathbf{E}^\varepsilon(0, \mathbf{x}_0) \\ & + \frac{1}{(b^0)^2} A \nabla_{\mathbf{x}} b(X^{1st}) \cdot \left[\Pi(\mathrm{e}^{\tau J} Y^{1st}) + A \mathrm{e}^{\tau J} \Pi (B(X^{1st}) J \mathbf{v}_0 \right] J \mathbf{v}_0. \end{aligned} \tag{2.40}$$

We now insert this expression in (2.39) to get

$$\mathbf{r}^{2nd}(\tau) := A B(X^{2nd}) J Y^{1st} + \frac{\varepsilon}{b^0} A \mathrm{e}^{-J\tau} \mathbf{E}^\varepsilon(0, X^{1st}) - \varepsilon L^{-1} \mathcal{T}^{2nd}. \tag{2.41}$$

We then get the following third order expansion for Y

$$Y(0,\tau) = \underline{Y}(0) + \mathbf{r}^{2nd}(\tau) + O(\varepsilon^3),$$

so that

$$Y(0,\tau) = Y^{2nd}(\tau) + O(\varepsilon^3), \tag{2.42}$$

where, using (2.29)

$$Y^{2nd}(\tau) := \mathbf{v}_0 + \mathbf{r}^{2nd}(\tau) - \mathbf{r}^{2nd}(0), \tag{2.43}$$

where $\mathbf{r}^{2nd}$ is given by (2.41) and where $X^{1st}, Y^{1st}, X^{2nd}, \mathcal{T}^{2nd}$ are given by (2.31), (2.34), (2.38), and (2.40).

2.4. **Proof of Proposition 2.1.** In this subsection, we prove that the time derivatives of $X(s,\tau)/\varepsilon$ and $Y(s,\tau)$ are uniformly bounded when the initial data is chosen following the Chapman-Enskog procedure presented previously, as stated in Proposition 2.1. Note that due to the $1/\varepsilon$ factor for X, its expansion has to be performed one order further as compared to the expansion of Y. The proof is an application of Lemma 2.3, where the time differentiation of the two-scale system (3.17) fits.

Proof. The time derivatives of the unknowns, denoted in this proof as $\tilde{X}(s,\tau) := \partial_s X(s,\tau)$, $\tilde{Y}(s,\tau) := \partial_s Y(s,\tau)$ satisfy

$$\partial_s \tilde{X} + \frac{1}{\varepsilon}\partial_\tau \tilde{X} = \frac{\mathrm{e}^{\tau J}}{b^0}\tilde{Y}, \tag{2.44}$$

$$\begin{aligned}\partial_s \tilde{Y} + \frac{1}{\varepsilon}\partial_\tau \tilde{Y} =& \frac{1}{\varepsilon}\left(\frac{b(X)}{b^0} - 1\right) J\tilde{Y} + \frac{1}{\varepsilon b^0}\nabla_{\mathbf{x}} b(X)\cdot \tilde{X} J Y \\ &+ \frac{\mathrm{e}^{-J\tau}}{b^0}\left(\frac{\partial_t \mathbf{E}^\varepsilon(s/b^0, X)}{b^0} + \nabla_{\mathbf{x}}\mathbf{E}^\varepsilon(s/b^0, X)\tilde{X}\right).\end{aligned} \tag{2.45}$$

With $X(0,\tau) = X^{1st}(\tau)$ (given by (2.30)-(2.31)) and $Y(0,\tau) = \mathbf{v}_0$ and using equation (2.13), we find the following initial data for the previous system

$$\begin{aligned}\partial_s X(0,\tau) = \tilde{X}(0,\tau) &= -\frac{1}{\varepsilon}\partial_\tau X^{1st}(\tau) + \frac{\mathrm{e}^{\tau J}}{b^0}\mathbf{v}_0 \\ &= -\frac{\mathrm{e}^{\tau J}}{b^0}\mathbf{v}_0 + \frac{\mathrm{e}^{\tau J}}{b^0}\mathbf{v}_0 = 0,\end{aligned} \tag{2.46}$$

$$\begin{aligned}\partial_s Y(0,\tau) = \tilde{Y}(0,\tau) &= -\frac{1}{\varepsilon}\partial_\tau \mathbf{v}_0 + \frac{1}{\varepsilon}\left(\frac{b(X^{1st})}{b^0} - 1\right) J\mathbf{v}_0 + \mathrm{e}^{-J\tau}\frac{\mathbf{E}^\varepsilon(0, X^{1st})}{b^0}, \\ = -&\left[\frac{\nabla_{\mathbf{x}} b(\mathbf{x}_0)}{b^0}\cdot J(\mathrm{e}^{\tau J} - I)\mathbf{v}_0 + O(\varepsilon)\right] J\mathbf{v}_0 + \mathrm{e}^{-J\tau}\frac{\mathbf{E}^\varepsilon(0, X^{1st})}{b^0} = O(1).\end{aligned} \tag{2.47}$$

Now we fix $\tau \in \mathbb{T}$ as a parameter and together with (2.18), we define

$$\tilde{X}_\tau(s) := \frac{1}{\varepsilon}\tilde{X}\left(s, \frac{s}{\varepsilon} + \tau\right), \quad \tilde{Y}_\tau(s) := \frac{e^{\tau J}}{b^0}\tilde{Y}\left(s, \frac{s}{\varepsilon} + \tau\right),$$

which solves

$$\begin{aligned}\dot{\tilde{X}}_\tau =& \frac{\mathrm{e}^{Js/\varepsilon}}{\varepsilon}\tilde{Y}_\tau, \\ \dot{\tilde{Y}}_\tau =& \frac{1}{\varepsilon}\left(\frac{b(X_\tau)}{b^0} - 1\right) J\tilde{Y}_\tau + \frac{e^{J\tau}}{(b^0)^2}\nabla_{\mathbf{x}} b(X_\tau)\cdot \tilde{X}_\tau J Y_\tau \\ &+ \frac{\mathrm{e}^{-Js/\varepsilon}}{(b^0)^2}\left(\frac{\partial_t \mathbf{E}^\varepsilon(s/b^0, X_\tau)}{b^0} + \varepsilon\nabla_{\mathbf{x}}\mathbf{E}^\varepsilon(s/b^0, X_\tau)\tilde{X}_\tau\right).\end{aligned}$$

We can apply Lemma 2.3 with $\mathcal{H} = L^\infty_\tau([0,2\pi])$ since all the assumptions of this lemma are fullfilled. Indeed, $\tilde{X}_\tau(0)$ and $\tilde{Y}_\tau(0)$ are uniformly bounded in ε, the functions X_τ and Y_τ enjoy some boundedness properties (thanks to Lemma 2.4) and the functions b and E are smooth. This enables to derive the following estimate

$$\frac{1}{\varepsilon}\|\partial_s X\|_{L^\infty_s(L^\infty_\tau)} + \|\partial_s Y\|_{L^\infty_s(L^\infty_\tau)} \le C_0.$$

We now deal with $W^{1,\infty}_\tau$ estimates. This is done by differentiating the above system with respect to τ. The so-obtained system is still of the form of the Lemma 2.3 and we have to check that the initial data remains bounded. Clearly the τ-derivative of $\tilde{X}(0,\tau)$ is equal to zero ; concerning the τ-derivative of $\tilde{Y}(0,\tau)$, we have

$$\partial_\tau \tilde{Y}(0,\tau) = \frac{1}{\varepsilon b^0}\nabla_{\mathbf{x}} b(X^{1st})\cdot \partial_\tau X^{1st} J\mathbf{v}_0 + \partial_\tau\left(\mathrm{e}^{-J\tau}\frac{\mathbf{E}^\varepsilon(0, X^{1st})}{b^0}\right).$$

From the definition (2.30)-(2.31) of $X^{1st}(0,\tau)$, we have $\partial_\tau X^{1st} = \frac{\varepsilon}{b^0}e^{\tau J}\mathbf{v}_0$ so that $\partial_\tau \tilde{Y}(0,\tau) = O(1)$. Then, using Lemma 2.3 with $\mathcal{H} = L^\infty_\tau([0,2\pi])$ ends the proof of (i).

Let us now prove (ii). We denote $\check{X} := \partial_s^2 X$, $\check{Y} := \partial_s^2 Y$ which are solutions of the following system

$$\begin{aligned}\partial_s \check{X} + \frac{1}{\varepsilon}\partial_\tau \check{X} =& \frac{e^{\tau J}}{b^0}\check{Y},\\ \partial_s \check{Y} + \frac{1}{\varepsilon}\partial_\tau \check{Y} =& \frac{1}{\varepsilon}\left(\frac{b(X)}{b^0} - 1\right) J\check{Y} + \frac{2}{\varepsilon b^0}\nabla_{\mathbf{x}} b(X)\cdot \tilde{X} J\tilde{Y}\\ &+ \frac{1}{\varepsilon b^0}\nabla_{\mathbf{x}} b(X)\cdot \check{X} JY + \frac{1}{\varepsilon b^0}\tilde{X}^T\nabla_{\mathbf{x}}^2 b(X)\tilde{X} JY\\ &+ \frac{e^{-J\tau}}{b^0}\left(\frac{\partial_t^2 \mathbf{E}^\varepsilon(s/b^0, X)}{(b^0)^2} + \frac{2}{b^0}\nabla_{\mathbf{x}}\partial_t \mathbf{E}^\varepsilon(s/b^0, X)\tilde{X}\right)\\ &+ \frac{e^{-J\tau}}{b^0}\left(\tilde{X}^T\nabla_{\mathbf{x}}^2 \mathbf{E}^\varepsilon(s/b^0, X)\tilde{X} + \nabla_{\mathbf{x}}\mathbf{E}^\varepsilon(s/b^0, X)\check{X}\right).\end{aligned}$$

In order to apply Lemma 2.3, we first check that the initial data for this system is uniformly bounded (in ε). To do so, we use the system (2.44)-(2.45) at $s = 0$ to obtain

$$\check{X}(0,\tau) = \partial_s \tilde{X}(0,\tau) = -\frac{1}{\varepsilon}\partial_\tau \tilde{X}(0,\tau) + \frac{e^{\tau J}}{b^0}\tilde{Y}(0,\tau). \tag{2.48}$$

Firstly, we find

$$\begin{aligned}\partial_s X(0,\tau) &= \tilde{X}(0,\tau) = -\frac{1}{\varepsilon}\partial_\tau X^{2nd}(\tau) + \frac{e^{\tau J}}{b^0}Y^{1st}(\tau)\\ &= -\frac{1}{\varepsilon}\partial_\tau X^{1st}(\tau) + \frac{e^{\tau J}}{b^0}v_0 + O(\varepsilon),\end{aligned}$$

which leads to $\tilde{X}(0,\tau) = O(\varepsilon)$ thanks to (2.46), so that we deduce $\frac{1}{\varepsilon}\partial_\tau \tilde{X}(0,\tau) = O(1)$. Concerning the second term in (2.48), we look at $\tilde{Y}(0,\tau)$

$$\begin{aligned}\partial_s Y(0,\tau) = \tilde{Y}(0,\tau) &= -\frac{1}{\varepsilon}\partial_\tau Y^{1st} + \frac{1}{\varepsilon}B(X^{2nd})JY^{1st} + \frac{e^{-J\tau}}{b^0}\mathbf{E}^\varepsilon(0, X^{2nd})\\ &= \frac{1}{\varepsilon}B(X^{2nd})JY^{1st} + O(1) = \frac{1}{\varepsilon b^0}\nabla_{\mathbf{x}} b(\mathbf{x}_0)\cdot(X^{2nd} - \mathbf{x}_0)JY^{1st} + O(1) = O(1),\end{aligned}$$

with $B(X) = \frac{b(X)}{b^0} - 1$. This enables to prove that $\check{X}(0,\tau)$ given by (2.48) is uniformly bounded.

We now focus on $\check{Y}(0,\tau)$ which is given by

$$\begin{aligned}\partial_s^2 Y(0,\tau) = \check{Y}(0,\tau) =& \frac{1}{\varepsilon}B(X^{2nd})J\tilde{Y}(0,\tau) + \frac{1}{\varepsilon b^0}\nabla_{\mathbf{x}} b(X^{2nd})\cdot \tilde{X}(0,\tau)JY^{1st}\\ &+ \frac{e^{-J\tau}}{b^0}\left(\frac{\partial_t \mathbf{E}^\varepsilon(0, X^{2nd})}{b^0} + \nabla_{\mathbf{x}}\mathbf{E}^\varepsilon(0, X^{2nd})\tilde{X}(0,\tau)\right) - \frac{1}{\varepsilon}\partial_\tau \tilde{Y}(0,\tau)\\ =& -\frac{1}{\varepsilon}\partial_\tau \tilde{Y}(0,\tau) + O(1).\end{aligned}$$

Let us now look at $\partial_\tau \tilde{Y}(0,\tau)$. First, we have

$$\tilde{Y}(0,\tau) = \partial_s Y(0,\tau) = -\frac{1}{\varepsilon}\partial_\tau Y^{1st} + \frac{1}{\varepsilon}B(X^{2nd})JY^{1st} + \frac{e^{-\tau J}}{b^0}\mathbf{E}^\varepsilon(0, X^{2nd}).$$

We want to prove that $\tilde{Y}(0,\tau) = O(\varepsilon)$ to ensure $\check{Y}(0,\tau) = O(1)$. Using (2.34), we have

$$\partial_\tau Y^{1st}(0,\tau) = B(X^{1st})J\mathbf{v}_0 + \varepsilon\frac{e^{-\tau J}}{b^0}\mathbf{E}^\varepsilon(0,\mathbf{x}_0).$$

Injecting this last identity in the expression of $\tilde{Y}(0,\tau)$ leads to

$$\begin{aligned}\tilde{Y}(0,\tau) &= -\frac{1}{\varepsilon}\left[B(X^{1st})J\mathbf{v}_0 + \varepsilon\frac{e^{-\tau J}}{b^0}\mathbf{E}^\varepsilon(0,\mathbf{x}_0)\right] + \frac{1}{\varepsilon}B(X^{2nd})JY^{1st} + \frac{e^{-\tau J}}{b^0}\mathbf{E}^\varepsilon(0, X^{2nd})\\ &= -\frac{1}{\varepsilon}B(X^{1st})J\mathbf{v}_0 + \frac{1}{\varepsilon}B(X^{1st} + O(\varepsilon^2))J(\mathbf{v}_0 + O(\varepsilon)) + O(\varepsilon)\\ &= O(\varepsilon).\end{aligned}$$

Hence we have $\check{Y}(0,\tau)=O(1)$.

Again, considering new unknown $\frac{1}{\varepsilon}\check{X}(s,\frac{s}{\varepsilon}+\tau)$ and $\frac{e^{\tau J}}{b}\check{Y}(s,\frac{s}{\varepsilon}+\tau)$ enables to recast the previous system so that, using the previous estimates, we can use Lemma 2.3 with $\mathcal{H}=L^\infty_\tau([0,2\pi])$ provided that the initial data $\frac{1}{\varepsilon}\check{X}(0,\tau)=O(1)$. Then, we compute

$$\frac{1}{\varepsilon}\check{X}(0,\tau)=-\frac{1}{\varepsilon^2}\partial_\tau\tilde{X}(0,\tau)+\frac{1}{\varepsilon b^0}\mathrm{e}^{\tau J}\tilde{Y}(0,\tau)=-\frac{1}{\varepsilon^2}\partial_\tau\tilde{X}^{2nd}+\frac{1}{\varepsilon b^0}\mathrm{e}^{\tau J}\tilde{Y}^{1st}.$$

We focus on the first term

$$\begin{aligned}-\frac{1}{\varepsilon^2}\partial_\tau\tilde{X}^{2nd} &= -\frac{1}{\varepsilon^2 b^0}\partial_\tau(\mathrm{e}^{\tau J}Y^{1st})+\frac{1}{\varepsilon^2 b^0}\mathrm{e}^{\tau J}\Pi B(X^{1st})J\mathbf{v}_0+\frac{1}{\varepsilon^2 b^0}\partial_\tau(\mathrm{e}^{\tau J}Y^{1st})\\ &= -\frac{1}{\varepsilon^2 b^0}\mathrm{e}^{\tau J}\Pi B(X^{1st})J\mathbf{v}_0.\end{aligned}$$

Then, we compute the second term

$$\begin{aligned}\frac{1}{\varepsilon b^0}\mathrm{e}^{\tau J}\tilde{Y}^{1st} &= \frac{1}{\varepsilon b^0}\mathrm{e}^{\tau J}\Big[-\frac{1}{\varepsilon}\partial_\tau Y^{1st}+\frac{1}{\varepsilon}B(X^{2nd})JY^{1st}+\frac{1}{b^0}\mathrm{e}^{-\tau J}\mathbf{E}^\varepsilon(0,X^{2nd})\Big]\\ &= -\frac{1}{\varepsilon^2 b^0}\mathrm{e}^{\tau J}\Big[(I-\Pi)B(X^{1st})J\mathbf{v}_0+\frac{\varepsilon}{b^0}\mathrm{e}^{-\tau J}\mathbf{E}^\varepsilon(0,\mathbf{x}_0)\Big]\\ &\quad+\frac{1}{\varepsilon^2 b^0}\mathrm{e}^{\tau J}B(X^{2nd})JY^{1st}+\frac{1}{\varepsilon(b^0)^2}\mathbf{E}^\varepsilon(0,X^{2nd})\\ &= \frac{1}{\varepsilon^2 b^0}\mathrm{e}^{\tau J}\Big[-(I-\Pi)B(X^{1st})J\mathbf{v}_0+B(X^{2nd})JY^{1st}\Big]+\frac{1}{\varepsilon(b^0)^2}(\mathbf{E}^\varepsilon(0,X^{2nd})-\mathbf{E}^\varepsilon(0,\mathbf{x}_0))\\ &= \frac{1}{\varepsilon^2 b^0}\mathrm{e}^{\tau J}\Big[-(I-\Pi)B(X^{1st})J\mathbf{v}_0+B(X^{2nd})JY^{1st}\Big]+O(1).\end{aligned}$$

Gathering the two term leads to

$$\frac{1}{\varepsilon}\check{X}(0,\tau)=-\frac{1}{\varepsilon^2 b^0}\Big[-B(X^{1st})J\mathbf{v}_0+B(X^{2nd})JY^{1st}\Big]=\frac{B(X^{1st})}{\varepsilon^2 b^0}J(\mathbf{v}_0-Y^{1st})+O(1)=O(1),$$

since $X^{2nd}=X^{1st}+O(\varepsilon^2)$. Similar computations for $\partial_\tau\check{X}$ and $\partial_\tau\check{Y}$ leads to the required estimate. □

2.5. **Numerical illustrations.** To end this section, we illustrate the effect of the preparation of the initial data on the behaviour of the time derivative of X and Y. To do so, we consider an example of a single particle characteristics (2.2) with initial condition

$$\mathbf{x}_0=\begin{pmatrix}10\\1.3\end{pmatrix},\quad \mathbf{v}_0=\begin{pmatrix}4.9\\-2.1\end{pmatrix},$$

and

$$\begin{aligned}&b(\mathbf{x})=1+\sin(x_1)\sin(x_2)/2,\quad \mathbf{E}^\varepsilon(t,\mathbf{x})=\begin{pmatrix}E_1(\mathbf{x})\\E_2(\mathbf{x})\end{pmatrix}(1+\sin(t)/2),\\ &E_1(\mathbf{x})=\cos(x_1/2)\sin(x_2)/2,\quad E_2(\mathbf{x})=\sin(x_1/2)\cos(x_2).\end{aligned}\tag{2.49}$$

In Figure 1, we plot the time history of $\partial_s X$, $\partial_s Y$, $\partial_s^2 X$ and $\partial_s^2 Y$ (by an accurate numerical solver) under norm

$$\|X(t,\cdot)\|_{L^2_\tau}:=\frac{1}{2}\left(\|X_1(t,\cdot)\|_{L^2_\tau}+\|X_2(t,\cdot)\|_{L^2_\tau}\right),\quad X=\begin{pmatrix}X_1\\X_2\end{pmatrix},$$

for different initial data (first order initial data $(X^{1st},\mathbf{v}_0)$ with X^{1st} given by (2.31) and second order initial data (X^{2nd},Y^{1st}) with X^{2nd} given by (2.38) and Y^{1st} given by (2.34)). From the numerical results in Figure 1, we see that the initial data (X^{2nd},Y^{1st}) is able to provide the theoretical bound (2.6), while $(X^{1st},\mathbf{v}_0)$ is only enough to get (2.5). The results confirm Proposition 2.1 and illustrate the importance of the constructed initial data for the two-scale system.

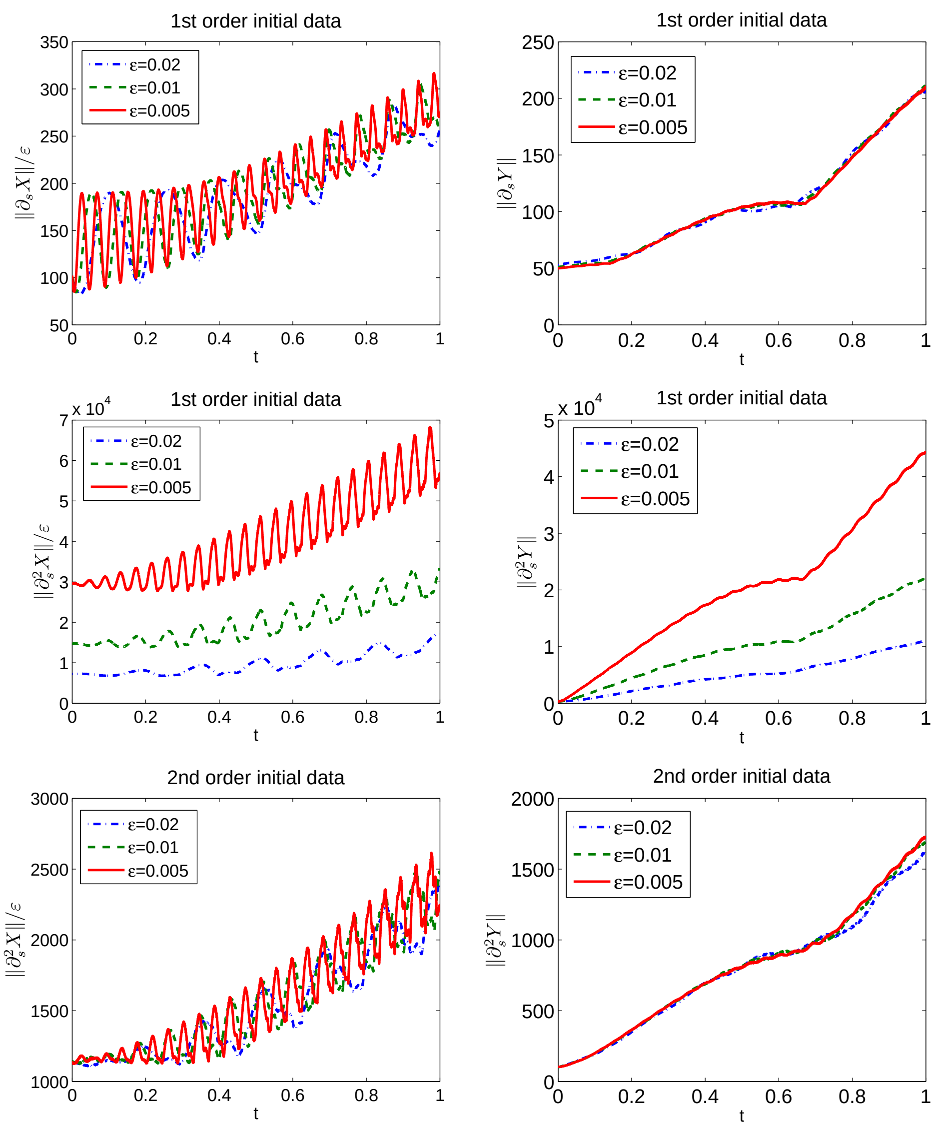

FIGURE 1. Time history of the norm of $\partial_s X/\varepsilon$, $\partial_s Y$ (first row) and $\partial_s^2 X/\varepsilon$, $\partial_s^2 Y$ (second and third rows) under first order initial data $(X^{1st}, \mathbf{v}_0)$ and respectively second order initial data (X^{2nd}, Y^{1st}).

3. NUMERICAL METHOD

This section is devoted to the construction of numerical schemes for the two-scaled system (2.13). We will perform the analysis of a first order numerical scheme: we will prove that this numerical scheme enjoy the uniform accuracy property with respect to ε. In addition, we will prove that the scheme is able to reproduce the confinement property (2.16) at the discrete level. Then, we will propose a strategy to reach the second order accuracy and to handle the coupling with Poisson equation.

Let $\Delta t > 0$ be the time step and denote $t_n = n\Delta t$ for $n \geq 0$ as the discretisation of the t-variable. For each particle $1 \leq k \leq N_p$, the discretisation of the scaled time s-variable is consequently as

$$\Delta s_k = b_k^0 \Delta t, \quad s_k^n = n\Delta s_k, \quad n = 0, 1, \ldots.$$

We certainly omit this subscript k for brevity, i.e. $\Delta s = \Delta s_k,\ s_n = s_k^n$. Denote the numerical solution as

$$X_k^n(\tau) \approx X_k(s_n,\tau), \quad Y_k^n(\tau) \approx Y_k(s_n,\tau), \quad n = 0,1,\dots,$$

and choose $X_k^0(\tau) = X_k(0,\tau)$, $Y_k^0(\tau) = Y_k(0,\tau)$.

3.1. First order numerical scheme.

A first order implicit-explicit (IMEX1) finite difference scheme reads for $n \geq 0$,

$$\frac{X_k^{n+1} - X_k^n}{\Delta s} + \frac{1}{\varepsilon}\partial_\tau X_k^{n+1} = \frac{\mathrm{e}^{\tau J}}{b_k^0} Y_k^{n+1}, \tag{3.1a}$$

$$\frac{Y_k^{n+1} - Y_k^n}{\Delta s} + \frac{1}{\varepsilon}\partial_\tau Y_k^{n+1} = \frac{1}{\varepsilon}\left(\frac{b(X_k^n)}{b_k^0} - 1\right) J Y_k^n + \mathrm{e}^{-J\tau}\frac{\mathbf{E}^\varepsilon(t_n, X_k^n)}{b_k^0}. \tag{3.1b}$$

In the Fourier space in τ, the above scheme is easily diagonalized. By discretizing the τ-direction as $\tau_j = j\Delta\tau, j = 0,\dots,N_\tau$ with $\Delta\tau = 2\pi/N_\tau$, N_τ being some positive even integer, one can use the Fourier transform in τ to get a fully discretized scheme. By doing so, let us remark that the IMEX scheme (3.1) is explicit from a computational point of view and the error in τ is uniformly (with respect to ε) spectrally uniform.

By assuming that $\mathbf{E}^\varepsilon(t,\mathbf{x})$ and $b(\mathbf{x})$ are smooth given functions, we analyse the first order IMEX scheme (3.1) for which we have the following uniform convergence results.

Theorem 3.1. *Under the assumptions in Proposition 2.1 for the two-scaled system (2.13), consider the first order IMEX1 scheme (3.1) for solving (2.13) with the second order initial data* $X_k^0(\tau) = X_k^{2nd}(\tau)$ *given by* (2.38) *and* $Y_k^0(\tau) = Y_k^{1st}(\tau)$ *given by* (2.34). *There exist constants* $C_0, C_1, C_2 > 0$ *independent of* ε, *such that when* $0 < \Delta s \leq C_0$ *we have*

$$\frac{1}{\varepsilon}\|X_k^n - X_k(s_n,\cdot)\|_{L_\tau^\infty} + \|Y_k^n - Y_k(s_n,\cdot)\|_{L_\tau^\infty} \leq C_1\Delta s, \quad 0 \leq n \leq \frac{S_k}{\Delta s}, \tag{3.2}$$

and

$$\|X_k^n - \mathbf{x}_{k,0}\|_{L_\tau^\infty} \leq C_2\varepsilon, \tag{3.3a}$$

$$\|Y_k^n\|_{L_\tau^\infty} \leq \|Y_k\|_{L_s^\infty(L_\tau^\infty)} + 1, \quad 0 \leq n \leq \frac{S_k}{\Delta s}. \tag{3.3b}$$

The error estimate shows that the scheme with well-prepared initial data offers super-convergence in $\mathbf{x}_k$. As a consequence, this super-convergence is also true for space dependent macroscopic quantities such as $\rho^\varepsilon(t,\mathbf{x})$. The estimate (3.3) indicates the confinement property at the discrete level.

We are going to prove this theorem by first introducing two lemmas concerning local truncation error and error propagation. To simplify the notations, we will always use C to denote a positive constant independent of $\Delta s, n$ or ε and it could change from line to line. We shall omit the subscript k in the following for simplicity.

Firstly, we define the local truncation error for the IMEX scheme (3.1) as

$$\xi_X^n(\tau) := \frac{X(s_{n+1},\tau) - X(s_n,\tau)}{\Delta s} + \frac{1}{\varepsilon}\partial_\tau X(s_{n+1},\tau) - \frac{\mathrm{e}^{\tau J} Y(s_{n+1},\tau)}{b^0}, \tag{3.4a}$$

$$\begin{aligned}\xi_Y^n(\tau) :=& \frac{Y(s_{n+1},\tau) - Y(s_n,\tau)}{\Delta s} + \frac{1}{\varepsilon}\partial_\tau Y(s_{n+1},\tau) - \mathrm{e}^{-\tau J}\frac{\mathbf{E}^\varepsilon(t_n, X(s_n,\tau))}{b^0}\\ &- \frac{1}{\varepsilon}\left(\frac{b(X(s_n,\tau))}{b^0} - 1\right) J Y(s_n,\tau), \quad \tau \in \mathbb{T}, \quad 0 \leq n \leq S_k/\Delta s.\end{aligned} \tag{3.4b}$$

We have

Lemma 3.2. *(Local error) Under the assumptions of Theorem 3.1, we have*

$$\frac{1}{\varepsilon}\|\xi_X^n\|_{W_\tau^{1,\infty}} + \|\xi_Y^n\|_{W_\tau^{1,\infty}} \leq C\Delta s, \quad 0 \leq n \leq S_k/\Delta s. \tag{3.5}$$

Proof. By Taylor's expansion, we have

$$X(s_n,\tau)=X(s_{n+1},\tau)-\Delta s\partial_s X(s_{n+1},\tau)+\Delta s^2\int_0^1\theta\partial_s^2X(s_n+\Delta s\,\theta,\tau)d\theta.$$

Inserting it into (3.4a) and then making use of the equation (2.13a), we get

$$\xi_X^n(\tau)=-\Delta s\int_0^1\theta\partial_s^2X(s_n+\Delta s\,\theta,\tau)d\theta.$$

Hence by Proposition 2.1, we get $\|\xi_X^n\|_{W_\tau^{1,\infty}}\leq\Delta s\|\partial_s^2X\|_{L_s^\infty(W_\tau^{1,\infty})}\leq C\varepsilon\Delta s$.

Similarly for the Y equation, we have Taylor's expansions,

$$\begin{aligned}
Y(s_n,\tau)&=Y(s_{n+1},\tau)-\Delta s\partial_s Y(s_{n+1},\tau)+\Delta s^2\int_0^1\theta\partial_s^2Y(s_n+\Delta s\,\theta,\tau)d\theta,\\
\mathbf{E}^\varepsilon(t_n,X(s_n,\tau))&=\mathbf{E}^\varepsilon(t_{n+1},X(s_{n+1},\tau))-\int_0^1\Big[\Delta t\partial_t\mathbf{E}^\varepsilon(t_n+\Delta t\theta,X(s_n,\tau))\\
&\quad+\Delta s\nabla_{\mathbf{x}}\mathbf{E}^\varepsilon(t_{n+1},X(s_n+\Delta s\theta,\tau))\partial_sX(s_n+\Delta s\theta,\tau)\Big]d\theta,\\
b(X(s_n,\tau))&=b(X(s_{n+1},\tau))-\Delta s\int_0^1\nabla_{\mathbf{x}}b(X(s_n+\Delta s\theta,\tau))\cdot\partial_sX(s_n+\Delta s\theta,\tau)d\theta.
\end{aligned}$$

Plugging them into (3.4b), we have

$$\begin{aligned}
\xi_Y^n(\tau)=&\partial_sY(s_{n+1},\tau)+\frac{1}{\varepsilon}\partial_\tau Y(s_{n+1},\tau)-\mathrm{e}^{-J\tau}\frac{\mathbf{E}^\varepsilon(t_{n+1},X(s_{n+1},\tau))}{b^0}\\
&-\frac{1}{\varepsilon}\left(\frac{b(X(s_{n+1},\tau))}{b^0}-1\right)JY(s_n,\tau)-\Delta s\int_0^1\theta\partial_s^2Y(s_n+\Delta s\theta,\tau)d\theta\\
&+\frac{\mathrm{e}^{-J\tau}}{b^0}\int_0^1\Big[\Delta t\partial_t\mathbf{E}^\varepsilon(t_n+\Delta t\theta,X(s_n,\tau))\\
&+\Delta s\nabla_{\mathbf{x}}\mathbf{E}^\varepsilon(t_{n+1},X(s_n+\Delta s\theta,\tau))\partial_sX(s_n+\Delta s\theta,\tau)\Big]d\theta,\\
&+\frac{\Delta s}{b^0\varepsilon}\int_0^1\nabla_{\mathbf{x}}b(X(s_n+\Delta s\theta,\tau))\cdot\partial_sX(s_n+\Delta s\theta,\tau)d\theta JY(s_n,\tau).
\end{aligned}$$

which with the Taylor's expansion

$$Y(s_n,\tau)=Y(s_{n+1},\tau)-\Delta s\int_0^1\partial_sY(s_n+\Delta s\theta,\tau)d\theta,$$

and the equation (2.13b) becomes

$$\begin{aligned}
\xi_Y^n(\tau)=&\frac{\Delta s}{\varepsilon}\left(\frac{b(X(s_{n+1},\tau))}{b^0}-1\right)J\int_0^1\partial_sY(s_n+\Delta s\theta,\tau)d\theta\\
&-\Delta s\int_0^1\theta\partial_s^2Y(s_n+\Delta s\theta,\tau)d\theta+\frac{\mathrm{e}^{-J\tau}}{b^0}\int_0^1\Big[\Delta t\partial_t\mathbf{E}^\varepsilon(t_n+\Delta t\theta,X(s_n,\tau))\\
&+\Delta s\nabla_{\mathbf{x}}\mathbf{E}^\varepsilon(t_{n+1},X(s_n+\Delta s\theta,\tau))\partial_sX(s_n+\Delta s\theta,\tau)\Big]d\theta,\\
&+\frac{\Delta s}{b^0\varepsilon}\int_0^1\nabla_{\mathbf{x}}b(X(s_n+\Delta s\theta,\tau))\cdot\partial_sX(s_n+\Delta s\theta,\tau)d\theta JY(s_n,\tau).
\end{aligned}$$

Hence again by Proposition 2.1 and Lemma 2.4, we get $\|\xi_Y^n\|_{W_\tau^{1,\infty}}\leq C\Delta s$. □

We now focus on the propagation error. First, we denote the error function as

$$\mathbf{e}_X^n(\tau):=X(s_n,\tau)-X^n(\tau),\quad \mathbf{e}_Y^n(\tau):=Y(s_n,\tau)-Y^n(\tau),\quad \tau\in\mathbb{T},\ 0\leq n\leq\frac{S_k}{\Delta s}.$$

It is obvious by the choice of the initial data that

$$\mathbf{e}_X^0(\tau)=\mathbf{e}_Y^0(\tau)=0.$$

Taking the difference between the local error (3.4) and scheme (3.1), we get the error equations

$$\frac{\mathbf{e}_X^{n+1}-\mathbf{e}_X^n}{\Delta s}+\frac{1}{\varepsilon}\partial_\tau \mathbf{e}_X^{n+1}=\frac{\mathrm{e}^{\tau J}}{b^0}\mathbf{e}_Y^{n+1}+\xi_X^n, \tag{3.6a}$$

$$\frac{\mathbf{e}_Y^{n+1}-\mathbf{e}_Y^n}{\Delta s}+\frac{1}{\varepsilon}\partial_\tau \mathbf{e}_Y^{n+1}=F^n+\xi_Y^n, \quad n\geq 0, \tag{3.6b}$$

where

$$\begin{aligned} F^n(\tau)=&\frac{1}{\varepsilon}\left[\left(\frac{b(X(s_n,\tau))}{b^0}-1\right)JY(s_n,\tau)-\left(\frac{b(X^n(\tau))}{b^0}-1\right)JY^n(\tau)\right]\\ &+\frac{\mathrm{e}^{-J\tau}}{b^0}\left[\mathbf{E}^\varepsilon(t_n,X(s_n,\tau))-\mathbf{E}^\varepsilon(t_n,X^n(\tau))\right]. \end{aligned} \tag{3.7}$$

In the following, for any τ-function $\varphi(\tau)$, its Fourier coefficients are defined by

$$\widehat{(\varphi)}_l=\frac{1}{2\pi}\int_0^{2\pi}e^{-il\tau}\varphi(\tau)d\tau. \tag{3.8}$$

Lemma 3.3. *(Error propagation) For the IMEX1 scheme (3.1), we have the following formula for the error function on the $l\in\mathbb{Z}$ Fourier coefficients in τ and for $n\geq 1$,*

$$\begin{aligned} \widehat{(\mathbf{e}_X^n)}_l=&\frac{\Delta s^2}{2b^0}\sum_{j=1}^n \alpha_{j,l}(I+iJ)\left[\widehat{(F^{n-j})}_{l+1}+\widehat{(\xi_Y^{n-j})}_{l+1}\right]+\Delta s\sum_{j=0}^{n-1}p_l^{j+1}\widehat{(\xi_X^{n-1-j})}_l\\ &+\frac{\Delta s^2}{2b^0}\sum_{j=1}^n \beta_{j,l}(I-iJ)\left[\widehat{(F^{n-j})}_{l-1}+\widehat{(\xi_Y^{n-j})}_{l-1}\right] \end{aligned} \tag{3.9a}$$

$$\widehat{(\mathbf{e}_Y^n)}_l=\Delta s\sum_{j=1}^n p_l^j\left[\widehat{(F^{n-j})}_l+\widehat{(\xi_Y^{n-j})}_l\right], \tag{3.9b}$$

where

$$\alpha_{j,l}=\frac{p_l^{j+1}p_{l+1}-p_lp_{l+1}^{j+1}}{p_l-p_{l+1}},\quad \beta_{j,l}=\frac{p_l^{j+1}p_{l-1}-p_lp_{l-1}^{j+1}}{p_l-p_{l-1}}\ \textit{and}\quad p_l:=\frac{1}{1+il\Delta s/\varepsilon},\quad l\in\mathbb{Z}.$$

Proof. Taking the Fourier transform (3.8) of (3.6), we have

$$\begin{aligned} &\frac{\widehat{(\mathbf{e}_X^{n+1})}_l-\widehat{(\mathbf{e}_X^n)}_l}{\Delta s}+\frac{il}{\varepsilon}\widehat{(\mathbf{e}_X^{n+1})}_l=\frac{\widehat{(\mathrm{e}^{\tau J}\mathbf{e}_Y^{n+1})}_l}{b^0}+\widehat{(\xi_X^n)}_l,\\ &\frac{\widehat{(\mathbf{e}_Y^{n+1})}_l-\widehat{(\mathbf{e}_Y^n)}_l}{\Delta s}+\frac{il}{\varepsilon}\widehat{(\mathbf{e}_Y^{n+1})}_l=\widehat{(F^n)}_l+\widehat{(\xi_Y^n)}_l,\quad l\in\mathbb{Z},\quad n\geq 0. \end{aligned}$$

Noting that

$$\widehat{(\mathrm{e}^{\tau J}\mathbf{e}_Y^n)}_l=\frac{1}{2}\left[(I+iJ)\widehat{(\mathbf{e}_Y^n)}_{l+1}+(I-iJ)\widehat{(\mathbf{e}_Y^n)}_{l-1}\right],$$

we have

$$\widehat{(\mathbf{e}_X^{n+1})}_l=p_l\widehat{(\mathbf{e}_X^n)}_l+\frac{p_l\Delta s}{2b^0}\left[(I+iJ)\widehat{(\mathbf{e}_Y^{n+1})}_{l+1}+(I-iJ)\widehat{(\mathbf{e}_Y^{n+1})}_{l-1}\right]+p_l\Delta s\widehat{(\xi_X^n)}_l, \tag{3.10a}$$

$$\widehat{(\mathbf{e}_Y^{n+1})}_l=p_l\widehat{(\mathbf{e}_Y^n)}_l+p_l\Delta s\left[\widehat{(F^n)}_l+\widehat{(\xi_Y^n)}_l\right],\quad l\in\mathbb{Z},\ n\geq 0. \tag{3.10b}$$

Let $n=0$ in the above relations, and then inserting (3.10b) into (3.10a), noting that $\mathbf{e}_X^0(\tau)=\mathbf{e}_Y^0(\tau)=0$, we get

$$\begin{aligned} \widehat{(\mathbf{e}_X^1)}_l=&\frac{p_l\Delta s^2}{2b^0}\left[p_{l+1}(I+iJ)(\widehat{(F^0)}_{l+1}+\widehat{(\xi_Y^0)}_{l+1})+p_{l-1}(\widehat{(F^0)}_{l-1}+\widehat{(\xi_Y^0)}_{l-1})\right]+p_l\Delta s\widehat{(\xi_X^0)}_l,\\ \widehat{(\mathbf{e}_Y^1)}_l=&p_l\Delta s\left[\widehat{(F^0)}_l+\widehat{(\xi_Y^0)}_l\right]. \end{aligned}$$

Therefore, the formula (3.9) with $n=1$ is true. Let us assume (3.9) is true for $1\leq m\leq n$ and we check the case $m=n+1$.

Plugging (3.9b) into (3.10b), we get

$$\begin{aligned}\widehat{(\mathbf{e}_Y^{n+1})}_l =&\Delta s \sum_{j=1}^{n} p_l^{j+1}\left[\widehat{(F^{n-j})}_l + \widehat{(\xi_Y^{n-j})}_l\right] + p_l\Delta s\left[\widehat{(F^n)}_l + \widehat{(\xi_Y^n)}_l\right]\\ =&\Delta s\sum_{j=1}^{n+1} p_l^j\left[\widehat{(F^{n+1-j})}_l + \widehat{(\xi_Y^{n+1-j})}_l\right]. \end{aligned}\tag{3.11}$$

Hence (3.9b) is checked. Next, plugging (3.11) and (3.9a) into (3.10a) leads to

$$\begin{aligned}\widehat{(\mathbf{e}_X^{n+1})}_l =&\frac{\Delta s^2}{2b^0}\sum_{j=1}^{n} p_l\alpha_{j,l}(I+iJ)\left[\widehat{(F^{n-j})}_{l+1} + \widehat{(\xi_Y^{n-j})}_{l+1}\right] + \Delta s\sum_{j=0}^{n-1} p_l^{j+2}\widehat{(\xi_X^{n-1-j})}_l\\ &+\frac{\Delta s^2}{2b^0}\sum_{j=1}^{n} p_l\beta_{j,l}(I-iJ)\left[\widehat{(F^{n-j})}_{l-1} + \widehat{(\xi_Y^{n-j})}_{l-1}\right] + p_l\Delta s\widehat{(\xi_Y^n)}_l\\ &+\frac{p_l\Delta s^2}{2b^0}(I+iJ)\sum_{j=1}^{n+1} p_{l+1}^j\left[\widehat{(F^{n+1-j})}_{l+1} + \widehat{(\xi_Y^{n+1-j})}_{l+1}\right]\\ &+\frac{p_l\Delta s^2}{2b^0}(I-iJ)\sum_{j=1}^{n+1} p_{l-1}^j\left[\widehat{(F^{n+1-j})}_{l-1} + \widehat{(\xi_Y^{n+1-j})}_{l-1}\right].\end{aligned}$$

First, we use the relation

$$\sum_{j=0}^{n-1} p_l^{j+2}\widehat{(\xi_X^{n-1-j})}_l + p_l\widehat{(\xi_Y^n)}_l = \sum_{j=0}^{n} p_l^{j+1}\widehat{(\xi_X^{n-j})}_l,$$

which enables to recover the second term of (3.9a) for $n+1$. Second, we remark than $p_l\alpha_{0,l}=0$ so that the first term in the previous expression of $\widehat{(\mathbf{e}_X^{n+1})}_l$ can be reformulated as

$$\sum_{j=1}^{n} p_l\alpha_{j,l}\left[\widehat{(F^{n-j})}_{l+1} + \widehat{(\xi_Y^{n-j})}_{l+1}\right] = \sum_{j=1}^{n+1}\frac{p_l^{j+1}p_{l+1} - p_l^2 p_{l+1}^j}{p_l - p_{l+1}}\left[\widehat{(F^{n+1-j})}_{l+1} + \widehat{(\xi_Y^{n+1-j})}_{l+1}\right].$$

Then, combining the latter with the term of the third line together with the following relation

$$\frac{p_l^{j+1}p_{l+1} - p_l^2p_{l+1}^j}{p_l - p_{l+1}} + p_l p_{l+1}^j = \frac{p_l^{j+1}p_{l+1} - p_l p_{l+1}^{j+1}}{p_l - p_{l+1}} = \alpha_{j,l},$$

leads to the first term (with $n+1$) of (3.9a). Similar arguments enable to recover the last term of (3.9a). Hence (3.9a) holds for $n+1$ and the induction proof is done so that the formula (3.9) holds for all $n \geq 1$. □

Lemma 3.4. *Let* $p_l = \frac{1}{1+il\Delta s/\varepsilon}, \forall l \in \mathbb{Z}$, *then the following estimates hold*

$$|p_l| \leq 1, \quad \forall l \in \mathbb{Z}, \quad \textit{and} \quad \Delta s|p_l| \leq \varepsilon, \quad \forall l \in \mathbb{Z}\backslash\{0\},$$

$$\Delta s\left|\frac{p_l^{j+1}p_{l\pm1} - p_l p_{l\pm1}^{j+1}}{p_l - p_{l\pm1}}\right| \leq C\varepsilon, \quad \forall l\in\mathbb{Z}, \forall j \in \mathbb{N}^\star,$$

where the constant $C>0$ *is independent of* $l, j, \Delta s$ *and* ε.

Proof. The first inequality is immediate. For the second one, we have $(\Delta s/\varepsilon)|p_l| = (\Delta s/\varepsilon)/(1+\Delta s^2/\varepsilon^2)^{1/2}$ and conclude owing that the function $f(a) = a/\sqrt{1+a^2}, a\geq 0$ is bounded (with $a = \Delta s/\varepsilon$).

Let consider the last inequality. Denoting again $a = \Delta s/\varepsilon$, we have

$$a\left|\frac{p_l^{j+1}p_{l\pm1} - p_l p_{l\pm1}^{j+1}}{p_l - p_{l\pm1}}\right| = a\left|\frac{p_l p_{l\pm1}}{p_l - p_{l\pm1}}\right| |p_l^j - p_{l\pm1}^j| = |p_l^j - p_{l\pm1}^j| \leq 2$$

since $a\left|\frac{p_l p_{l\pm1}}{p_l - p_{l\pm1}}\right| = 1$ and $|p_l|\leq 1$. □

3.2. **Proof of the convergence theorem.** Now with Lemmas 3.2-3.4, we give the proof of the convergence Theorem 3.1.

Proof of Theorem 3.1: We will proceed by an induction on n, by assuming that the following estimate holds for all $m = 0, \dots, n$

$$\frac{1}{\varepsilon}\|X_k^m - \mathbf{x}_{k,0}\|_{H^1_\tau} + \|Y_k^m\|_{H^1_\tau} \le \frac{1}{\varepsilon}\|X_k(s_m) - \mathbf{x}_{k,0}\|_{H^1_\tau} + \|Y_k(s_m)\|_{H^1_\tau} + 1, \tag{3.12}$$

and using the relations (3.9) on $\mathbf{e}_X^n$ and $\mathbf{e}_Y^n$.

Using Lemma 2.4, this implies in particular $\|Y_k^m\|_{H^1_\tau} \le C$. Then, we can deduce an estimate for the nonlinear part F^m given by (3.7)

$$\|F^m\|_{H^1_\tau} \le C\|\mathbf{e}_Y^m\|_{H^1_\tau} + \frac{C}{\varepsilon}\|\mathbf{e}_X^m\|_{H^1_\tau}, \quad 0 \le m \le n, \tag{3.13}$$

using again Lemma 2.4 and Sobolev embeddings. Finally, in view of deriving an estimate for e_X^{n+1} and e_Y^{n+1}, we use the Lemma 3.4 on the p_l coefficients to get from the error formula (3.9a) at $(n+1)$,

$$\begin{aligned}|\widehat{(\mathbf{e}_X^{n+1})}_l| \le& \Delta s\sum_{j=0}^{n}|\widehat{(\xi_X^{n-j})}_l| \\ &+ C\varepsilon\Delta s\sum_{j=0}^{n}\left[|\widehat{(F^{n-j})}_{l+1}| + |\widehat{(\xi_X^{n-j})}_{l+1} + |\widehat{(F^{n-j})}_{l-1}| + |\widehat{(\xi_X^{n-j})}_{l-1}|\right].\end{aligned} \tag{3.14}$$

Taking the square of (3.14) and using Cauchy-Schwarz inequality lead to

$$\begin{aligned}|\widehat{(\mathbf{e}_X^{n+1})}_l|^2 \le& C\Delta s\sum_{j=0}^{n}|\widehat{(\xi_X^{n-j})}_l|^2 \\ &+ C\varepsilon^2\Delta s\sum_{j=0}^{n}\left[|\widehat{(F^{n-j})}_{l+1}|^2 + |\widehat{(\xi_X^{n-j})}_{l+1}|^2 + |\widehat{(F^{n-j})}_{l-1}|^2 + |\widehat{(\xi_X^{n-j})}_{l-1}|^2\right].\end{aligned}$$

Then, to get H^1_τ estimate, we multiply by $(1, l^2)$, sum on $l \in \mathbb{Z}$ and add the two resulting equations so that, using Parseval identity, we obtain

$$\|\mathbf{e}_X^{n+1}\|^2_{H^1_\tau} \le C\Delta s\sum_{j=0}^{n}\|\xi_X^{n-j}\|^2_{H^1_\tau} + C\varepsilon^2\Delta s\sum_{j=0}^{n}\left[\|F^{n-j}\|^2_{H^1_\tau} + \|\xi_Y^{n-j}\|^2_{H^1_\tau}\right].$$

By the error formula (3.9b), we get by similar arguments

$$\|\mathbf{e}_Y^{n+1}\|^2_{H^1_\tau} \le C\Delta s\sum_{j=0}^{n}\left[\|F^{n-j}\|^2_{H^1_\tau} + \|\xi_Y^{n-j}\|^2_{H^1_\tau}\right].$$

Combining the two, we then have

$$\frac{1}{\varepsilon^2}\|\mathbf{e}_X^{n+1}\|^2_{H^1_\tau} + \|\mathbf{e}_Y^{n+1}\|^2_{H^1_\tau} \le C\Delta s\sum_{j=0}^{n}\left[\frac{1}{\varepsilon^2}\|\xi_X^j\|^2_{H^1_\tau} + \|\xi_Y^j\|^2_{H^1_\tau}\right] + C\Delta s\sum_{j=0}^{n}\|F^j\|^2_{H^1_\tau}.$$

Now inserting estimates (3.5) and (3.13), we get

$$\frac{1}{\varepsilon^2}\|\mathbf{e}_X^{n+1}\|^2_{H^1_\tau} + \|\mathbf{e}_Y^{n+1}\|^2_{H^1_\tau} \le C\Delta s^2 + C\Delta s\sum_{j=0}^{n}\left[\frac{1}{\varepsilon^2}\|\mathbf{e}_X^j\|^2_{H^1_\tau} + \|\mathbf{e}_Y^j\|^2_{H^1_\tau}\right],$$

and we conclude by using discrete Gronwall's lemma to get

$$\frac{1}{\varepsilon}\|\mathbf{e}_X^{n+1}\|_{H^1_\tau} + \|\mathbf{e}_Y^{n+1}\|_{H^1_\tau} \le C\Delta s.$$

As long as (3.12) is true, we then deduce

$$\frac{1}{\varepsilon}\|X_k^{n+1} - \mathbf{x}_{k,0}\|_{H^1_\tau} + \|Y_k^{n+1}\|_{H^1_\tau} \le \frac{1}{\varepsilon}\|X_k(s_{n+1}) - \mathbf{x}_{k,0}\|_{H^1_\tau} + \|Y_k(s_{n+1})\|_{H^1_\tau} + C\Delta s,$$

which completes the induction proof by considering $\Delta s \le \Delta s_0 = 1/C$. □

3.3. **Second order numerical scheme.** A second order scheme (IMEX2) for solving (2.13) could be written down as follows. For $n \geq 0$,

$$\frac{X_k^{n+1}-X_k^n}{\Delta s}+\frac{1}{2\varepsilon}\partial_\tau\left(X_k^{n+1}+X_k^n\right)=\frac{\mathrm{e}^{\tau J}}{b_k^0}Y_k^{n+1/2}, \tag{3.15a}$$

$$\begin{aligned}\frac{Y_k^{n+1}-Y_k^n}{\Delta s}+\frac{1}{2\varepsilon}\partial_\tau\left(Y_k^{n+1}+Y_k^n\right)=&\frac{1}{\varepsilon}\left(\frac{b(\overline{X}_k^{n+1/2})}{b_k^0}-1\right)JY_k^{n+1/2}\\&+\mathrm{e}^{-J\tau}\frac{\mathbf{E}^\varepsilon(t_{n+1/2},\overline{X}_k^{n+1/2})}{b_k^0}.\end{aligned} \tag{3.15b}$$

with

$$\begin{aligned}\overline{X}_k^{n+1/2}&=\frac{X_k^n+X_k^{n+1}}{2},\\ \frac{X_k^{n+1/2}-X_k^n}{\Delta s/2}+\frac{1}{\varepsilon}\partial_\tau X_k^{n+1/2}&=\frac{\mathrm{e}^{\tau J}}{b_k^0}Y_k^n,\\ \frac{Y_k^{n+1/2}-Y_k^n}{\Delta s/2}+\frac{1}{\varepsilon}\partial_\tau Y_k^{n+1/2}&=\frac{1}{\varepsilon}\left(\frac{b(X_k^n)}{b_k^0}-1\right)JY_k^n+\mathrm{e}^{-J\tau}\frac{\mathbf{E}^\varepsilon(t_{n+1/2},X_k^{n+1/2})}{b_k^0}.\end{aligned}$$

The above IMEX2 scheme is also explicit. From practical results (as can be seen in the next section), we observe that the IMEX2 with the 3rd order prepared initial data (derived in Appendix A) gives second order uniform accuracy. However, the rigorous error estimates would be more involved than the first order IMEX1 scheme and it is still under-going. We will address it in a future work.

3.4. **A strategy for the Vlasov-Poisson case.** When the Vlasov equation (1.1a) is coupled to Poisson equation, the electric field $\mathbf{E}^\varepsilon$ is a self-consistent field and the problem becomes nonlinear. Under PIC discretisation, $\mathbf{E}^\varepsilon$ in (2.2) is given by

$$\nabla_{\mathbf{x}}\cdot\mathbf{E}^\varepsilon(t,\mathbf{x})=\sum_{k=1}^{N_p}\omega_k\delta(\mathbf{x}-\mathbf{x}_k(t)),\quad t\geq 0,\ \mathbf{x}\in\mathbb{R}^2. \tag{3.16}$$

Hence by under the scale of time $s_j=b_jt$, the electric field evaluated at one particular particle $\mathbf{x}_j(t)$ $(1\leq j\leq N_p)$ solves (as we see in (2.8))

$$\nabla_{\mathbf{x}}\cdot\mathbf{E}^\varepsilon(s_j/b_j,\mathbf{x}_j(t))=\sum_{k=1}^{N_p}\omega_k\delta(\mathbf{x}_j(t)-\mathbf{x}_k(s_j/b_j)).$$

Each particle carries its own frequency and now all the particle are coupled to each other through Poisson equation, which as a result mixes all the frequencies. Thus, (2.8) is a multiple-frequency system with a large number N_p of degrees [9] and the proposed two-scale formulation is not rigorously working. Here, we give a practical strategy that works well based on our numerical experiments.

Note the above strategy relies on the key confinement property (see Lemma 2.2)

$$b(\tilde{\mathbf{x}}_k(s))-b_k^0=C(s)\varepsilon,\quad s>0,\ \ 1\leq k\leq N_p,$$

as well as the two-scale version in Lemma 2.3. In order to have a better control of $C(s)$ in the oscillatory case, we consider the scale of time (2.7) dynamically. Discretize time with $\Delta t>0$ and denote $t_n=n\Delta t$. For $n\geq 0$ and $t_n\leq t\leq t_{n+1}$, define

$$b_k^n=b(\mathbf{x}_k(t_n)),\quad t=t_n+\frac{s}{b_k^n},\quad \tilde{\mathbf{x}}_k(s)=\mathbf{x}_k(t), \tag{3.17}$$

and we solve

$$\dot{\tilde{\mathbf{x}}}_k(s) = \frac{\tilde{\mathbf{v}}_k(s)}{b_k^n}, \tag{3.18a}$$

$$\dot{\tilde{\mathbf{v}}}_k(s) = \frac{b(\tilde{\mathbf{x}}_k(s))}{\varepsilon b_k^n} J\tilde{\mathbf{v}}_k(t) + \frac{\mathbf{E}^\varepsilon(t_n + s/b_k^n, \tilde{\mathbf{x}}_k(s))}{b_k^n}, \quad 0 < s \leq b_k^n \Delta t, \tag{3.18b}$$

$$\tilde{\mathbf{x}}_k(0) = \mathbf{x}_k(t_n), \quad \tilde{\mathbf{v}}_k(0) = \mathbf{v}_k(t_n), \tag{3.18c}$$

for one step with $\Delta s = b_k^n \Delta t$. Again we isolate the leading order oscillation term, filter out this main oscillation (2.9) and then consider the two-scale formulation but leave the high-frequency character of the electric field part alone [14]. We then obtain

$$\partial_s X_k + \frac{1}{\varepsilon}\partial_\tau X_k = \frac{\mathrm{e}^{\tau J}}{b_k^n} Y_k, \quad 0 < s \leq \Delta s, \tag{3.19a}$$

$$\partial_s Y_k + \frac{1}{\varepsilon}\partial_\tau Y_k = \frac{1}{\varepsilon}\left(\frac{b(X_k)}{b_k^n} - 1\right) JY_k + \mathrm{e}^{-\tau J}\frac{\mathbf{E}^\varepsilon(t_n + s/b_k^n, X_k)}{b_k^n}. \tag{3.19b}$$

For the initial data, we formally choose $X_k(0,\tau) = X_k^{1st}(\tau)$, $Y_k(0,\tau) = Y_k^{1st}(\tau)$ given by (2.31) and (2.34) by replacing $\mathbf{x}_{k,0}$ and $\mathbf{v}_{k,0}$ with respectively $\mathbf{x}_k(t_n)$ and $\mathbf{v}_k(t_n)$. This initial data enables to offer second order uniform accuracy when an exponential integrator scheme (as in [15]) is used for (3.19).

We shall briefly derive the scheme. For the simplicity of notations, we put (3.19a)-(3.19b) into the following compact form:

$$\partial_s U_k(s,\tau) + \frac{1}{\varepsilon}\partial_\tau U_k(s,\tau) = F_k(s,\tau), \quad 0 < s \leq \Delta s, \ \tau \in \mathbb{T}, \tag{3.20}$$

where we denote

$$U_k(s,\tau) = \begin{pmatrix} X_k(s,\tau) \\ Y_k(s,\tau) \end{pmatrix}, \quad F_k(s,\tau) = \begin{pmatrix} F_{1,k}(s,\tau) \\ F_{2,k}(s,\tau) \end{pmatrix},$$

with

$$F_{1,k}(s,\tau) = \frac{\mathrm{e}^{\tau J}}{b_k^n} Y_k(s,\tau), \tag{3.21a}$$

$$F_{2,k}(s,\tau) = \frac{1}{\varepsilon}\left(\frac{b(X_k(s,\tau))}{b_k^n} - 1\right) JY_k(s,\tau) + \mathrm{e}^{-\tau J}\frac{\mathbf{E}^\varepsilon(t_n + s/b_k^n, X_k(s,\tau))}{b_k^n}. \tag{3.21b}$$

Applying Fourier transform in τ on (3.20)

$$U_k(s,\tau) = \sum_{l=-N_\tau/2}^{N_\tau/2-1} \widehat{(U_k)}_l(s)\mathrm{e}^{il\tau}, \qquad F_k(s,\tau) = \sum_{l=-N_\tau/2}^{N_\tau/2-1} \widehat{(F_k)}_l(s)\mathrm{e}^{il\tau},$$

and then by Duhamel's principle from 0 to Δs ($n \geq 0$),

$$\widehat{(U_k)}_l(\Delta s) = \mathrm{e}^{-\frac{il\Delta s}{\varepsilon}}\widehat{(U_k)}_l(0) + \int_0^{\Delta s} \mathrm{e}^{-\frac{il}{\varepsilon}(\Delta s - \theta)}\widehat{(F_k)}_l(\theta)d\theta.$$

A first order uniformly accurate scheme, shorted as EI1 in the following, is obtained as,

$$\begin{aligned} \widehat{(U_k)}_l(\Delta s) &\approx \mathrm{e}^{-\frac{il\Delta s}{\varepsilon}}\widehat{(U_k)}_l(0) + \int_0^{\Delta s} \mathrm{e}^{-\frac{il}{\varepsilon}(\Delta s - \theta)}\widehat{(F_k)}_l(0)d\theta \\ &\approx \mathrm{e}^{-\frac{il\Delta s}{\varepsilon}}\widehat{(U_k)}_l(0) + p_l^E\widehat{(F_k)}_l(0), \end{aligned}$$

where

$$p_l^E := \int_0^{\Delta s} \mathrm{e}^{-\frac{il}{\varepsilon}(\Delta s - \theta)}d\theta = \begin{cases} \dfrac{i\varepsilon}{l}\left(\mathrm{e}^{-\frac{il\Delta s}{\varepsilon}} - 1\right), & l \neq 0, \\ \Delta s, & l = 0. \end{cases}$$

A second order scheme, shorted as EI2, is given as,

$$\begin{aligned}\widehat{(U_k)}_l(\Delta s) &\approx \mathrm{e}^{-\frac{il\Delta s}{\varepsilon}}\widehat{(U_k)}_l(0) + \int_0^{\Delta s} \mathrm{e}^{-\frac{il}{\varepsilon}(\Delta s-\theta)}\left(\widehat{(F_k)}_l(0) + \theta\frac{d}{ds}\widehat{(F_k)}_l(0)\right)d\theta \\ &\approx \mathrm{e}^{-\frac{il\Delta s}{\varepsilon}}\widehat{(U_k)}_l(0) + p_l^E\widehat{(F_k)}_l(s_n) + q_l^E\frac{1}{\Delta s}\left(\widehat{(F_k^*)}_l - \widehat{(F_k)}_l(0)\right),\end{aligned}$$

where

$$q_l^E := \int_0^{\Delta s} \mathrm{e}^{-\frac{il}{\varepsilon}(\Delta s-\theta)}\theta d\theta = \begin{cases}\dfrac{\varepsilon}{l^2}\left(\varepsilon - \varepsilon\mathrm{e}^{-\frac{il\Delta s}{\varepsilon}} - il\Delta s\right), & l \neq 0,\\ \dfrac{\Delta s^2}{2}, & l = 0.\end{cases}$$

and

$$\begin{aligned}\widehat{(U_k)}_l^* &= \mathrm{e}^{-\frac{il\Delta s}{\varepsilon}}\widehat{(U_k)}_l(0) + p_l^E\widehat{(F_k)}_l(0),\\ F_k^*(\tau) &= \begin{pmatrix}\mathrm{e}^{\tau J}Y_k^*(\tau)/b_k^n\\ \frac{1}{\varepsilon}\left(b(X_k^*(\tau))/b_k^n - 1\right)JY_k^*(\tau) + \mathrm{e}^{-\tau J}\mathbf{E}^\varepsilon(t_n + \Delta s/b_k^n, X_k^*(\tau))/b_k^n\end{pmatrix}.\end{aligned}$$

Suppose now we have computed numerically $X_k(\Delta s, \tau)$ as the two-scale solution for system (3.18), we update the electric field for the next time level t_{n+1} as

$$\nabla_{\mathbf{x}} \cdot \mathbf{E}^\varepsilon(t_{n+1}, \mathbf{x}) = \sum_{k=1}^{N_p} \omega_k \delta(\mathbf{x} - X_k(\Delta s, \Delta s/\varepsilon)), \qquad \mathbf{x} \in \mathbb{R}^2.$$

Remark 3.5. The technique and algorithm developed in this paper could be extended to the 3D Vlasov equation case with a full external varying magnetic field, but it is more difficult and involving. The confinement property is not true in the direction parallel to the magnetic field.

4. Numerical results

This section is devoted to numerical illustrations of the numerical schemes introduced above. We consider (1.1) with the following initial data

$$f_0(\mathbf{x}, \mathbf{v}) = \frac{1}{4\pi}\left(1 + \sin(x_2) + \eta\cos(kx_1)\right)\left(\mathrm{e}^{-\frac{(v_1+2)^2+v_2^2}{2}} + \mathrm{e}^{-\frac{(v_1-2)^2+v_2^2}{2}}\right), \tag{4.1}$$

with $\mathbf{x} = (x_1, x_2)$ and $\mathbf{v} = (v_1, v_2)$ and the non-homogeneous magnetic field

$$b(\mathbf{x}) = 1 + \sin(x_1)\sin(x_2)/2,$$

to test convergence order. Note the initial data we considered here is out of the equilibrium with respect to the stiffest term in the Vlasov equation (1.1). Indeed, f_0 in (4.1) depends on the polar velocity angle and our numerical strategy never requires the initial value of the PDE being well prepared. The spatial domain is $\mathbf{x} = (x_1, x_2) \in \Omega = [0, 2\pi/k] \times [0, 2\pi]$ for some $k, \eta > 0$. We choose $\eta = 0.05, k = 0.5$ and discretize Ω with 64 points in x_1-direction and 32 points in x_2-direction. As a diagnostic, we consider the following two quantities:

$$\begin{aligned}\rho^\varepsilon(t, \mathbf{x}) &= \int_{\mathbb{R}^2} f^\varepsilon(t, \mathbf{x}, \mathbf{v})d\mathbf{v}, \qquad \mathbf{x} \in \Omega,\\ \rho_{\mathbf{v}}^\varepsilon(t, \mathbf{x}) &= \int_{\mathbb{R}^2} |\mathbf{v}|^2 f^\varepsilon(t, \mathbf{x}, \mathbf{v})d\mathbf{v}.\end{aligned}$$

We then compute the relative errors of the different numerical schemes with respect to ρ^ε and $\rho_{\mathbf{v}}^\varepsilon$ at the final time $t_f = 1$ in maximum space norm. We numerically solve (1.1) with two configurations. For the first one, we consider an external electric field given by

$$\begin{aligned}\mathbf{E}^\varepsilon(t, \mathbf{x}) &= \begin{pmatrix}E_1(\mathbf{x})\\ E_2(\mathbf{x})\end{pmatrix}(1 + \sin(t)/2),\\ E_1(\mathbf{x}) &= \cos(x_1/2)\sin(x_2)/2, \quad E_2(\mathbf{x}) = \sin(x_1/2)\cos(x_2),\end{aligned}$$

which will be addressed as 'given E' in the numerical results. For the second case, we consider the nonlinear Vlasov-Poisson equation (1.1)-(1.3). The reference solution is obtained by using a fourth order Runge-Kutta method on the original problem (2.2) with step size $\Delta t = 10^{-6}$.

For the PIC method, we choose $N_p = 204800$ particles and the projection of the particles on the uniform spatial grid is done by quintic splines. The time step Δs is determined by fixing Δt (recall the relation $s = b_k^0 t$ and $\Delta s = b_k^0 \Delta t$) so that after N time steps (such that $t_f = N\Delta t$), every particles stop at the same time t_f. Finally, we denote by N_τ the number of grid points in the τ-direction: $\Delta\tau = 2\pi/N_\tau$.

In the sequel, second order initial data will refer to (X_k^{2nd}, Y_k^{1st}) with X_k^{2nd} given by (2.38) and Y_k^{1st} given by (2.34), whereas third order initial data will refer to (X_k^{3rd}, Y_k^{2nd}) with X_k^{3rd} given by (A.1) and Y_k^{2nd} given by (2.43).

External electric field. We first study the 'given E' case. In Figure 2, the errors (in L_t^∞ norm) in time of the IMEX1 scheme in ρ^ε with second order initial data are displayed for different values of ε. As shown in the numerical analysis (see Proposition 2.1 and Theorem 3.2), the scheme IMEX1 has uniform first order accuracy in time. Moreover, we can observe that the error decreases as ε goes to zero, in agreement with theoretical results.

In Figure 3, the errors (in L_t^∞ norm) in time of the IMEX1 scheme with second order initial data is plotted (under $N_\tau = 64$) regarding the quantities $\rho^\varepsilon/\varepsilon$ and $\rho^\varepsilon_{\mathbf{v}}$. We can observe the curves are almost superimposed confirming the theoretical error estimates derived previously. For $\rho^\varepsilon_{\mathbf{v}}$, since $\mathbf{v}$ does not enjoy the super convergence, so we expect first order uniform accuracy for $\rho_{\mathbf{v}}$.

It is important to check that a few number of points in τ are sufficient to get a good accuracy, since τ is an additional variable compared to the original model. The influence of the discretization in the τ direction of the IMEX1 (using $\Delta t = 10^{-5}$) is presented in Figure 4. We computed the difference between the numerical solution obtained with several N_τ and the one using $N_\tau = 64$, for the two quantities ρ^ε and $\rho^\varepsilon_{\mathbf{v}}$. The discretization error in τ has a spectral behavior with respect to N_τ, and when ε becomes small, we observe that the method reaches machine accuracy with very few number of grid points (typically $N_\tau = 8$ is sufficient when $\varepsilon = 10^{-3}$).

Next, we study the convergence of the second order IMEX2 scheme with third order initial data. $N_\tau = 64$ is fixed for the study. In Figures 5-7, we can see second order uniform accuracy of the scheme with respect to ε, regarding both $\rho^\varepsilon/\varepsilon$ and $\rho^\varepsilon_{\mathbf{v}}$.

We also study the convergence rate of the Vlasov equation (1.1) to the asymptotic model (derived in Appendix B) on the characteristics level when $\varepsilon \to 0$. To do so, we measure the difference between the solution of (1.1) for several ε and the one obtained with $\varepsilon = 10^{-4}$. In Figure 11, we show the convergence of the model (1.1) in the limit regime (with $\Delta t = 5^{-3}$), for which the rate is equal to one. Finally, we study the dynamics of the solution for a fixed $\varepsilon = 0.1$, aiming to see the effect from the non-constant magnetic field. The quantity $\rho^\varepsilon(t, \mathbf{x})$ is plotted as a function of $\mathbf{x}$ at different times in Figure 8 (with $\Delta t = 5^{-3}$).

Vlasov-Poisson case. For the Vlasov-Poisson case, we apply the strategy presented in subsection 3.4, namely the dynamical scaling EI2 scheme with initial data (X_k^{1st}, Y_k^{1st}). In Figure 9, we show the relative error (under $N_\tau = 64$) in time regarding both ρ^ε and $\rho^\varepsilon_{\mathbf{v}}$ in maximum norm. For a long-time diagnostic test of the scheme, we consider the energy of the Vlasov-Poisson equation which is conserved as

$$H(t) := \frac{1}{2}\int_{\mathbb{R}^2}\int_\Omega |\mathbf{v}|^2 f^\varepsilon(t, \mathbf{x}, \mathbf{v})d\mathbf{x}d\mathbf{v} + \frac{1}{2}\int_\Omega |\mathbf{E}^\varepsilon(t, \mathbf{x})|^2 d\mathbf{x} \equiv H(0).$$

We compute the numerical energy $H(t)$ by the EI2 scheme with $\Delta t = 0.05,\ N_\tau = 16$. In Figure 10, we show the relative energy error $|H(t) - H(0)|/H(0)$ till $t_f = 100$ for different values of ε (under $N_\tau = 32$). From the numerical results for the Vlasov-Poisson case, we see that the proposed strategy shows a promising performance. The errors in both position $\mathbf{x}$ and velocity $\mathbf{v}$ converge almost in a uniformly second order rate, although the super convergence is gone in this nonlinear configuration. The energy error of the method in long time is also uniform in terms of $0 < \varepsilon \leq 1$, though there is a linear drift. Compared to the scheme proposed in [19] which is asymptotic preserving to a gyrokinetic model in the limit $\varepsilon \to 0$, our method captures all the information including the fast

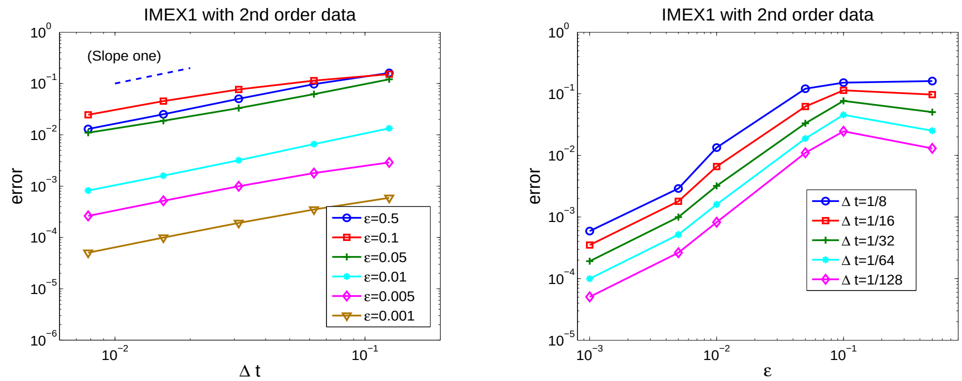

FIGURE 2. Temporal error of IMEX1 with second order initial data (X_k^{2nd}, Y_k^{1st}) for given E case: relative maximum error in ρ^ε.

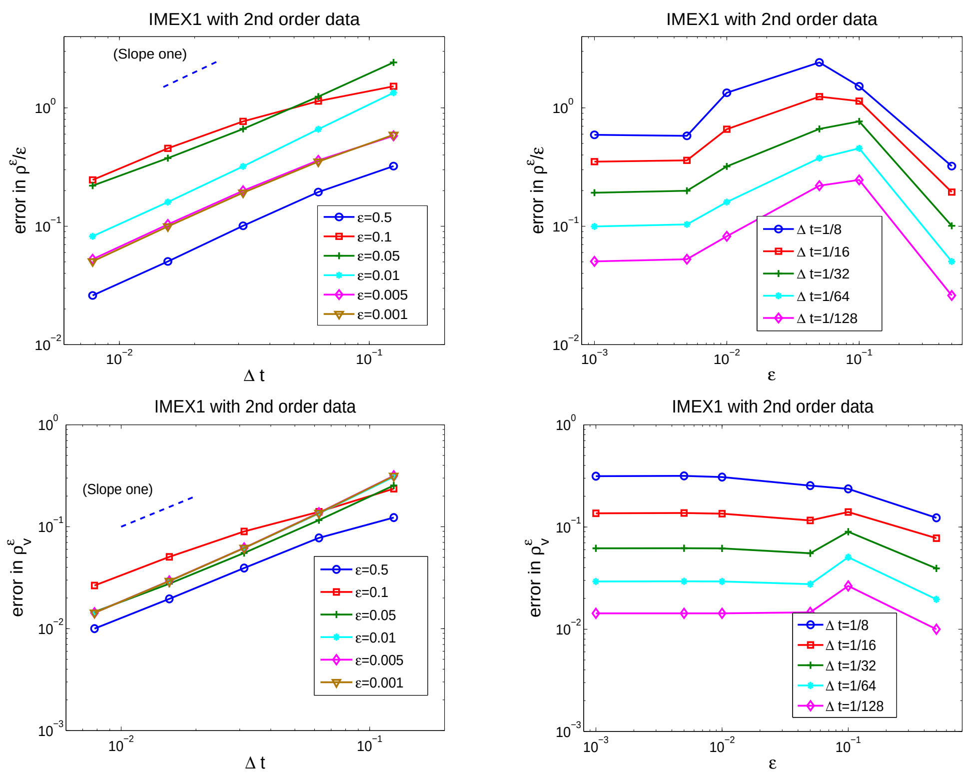

FIGURE 3. Temporal error of IMEX1 with second order initial data (X_k^{2nd}, Y_k^{1st}) for given E case: relative maximum error in $\rho^\varepsilon/\varepsilon$ (first row) and in $\rho^\varepsilon_{\mathbf{v}}$ (second row).

and slow dynamics of the Vlasov-Poisson model (1.1) in a uniformly accurate way. In addition, the strategy proposed in [22] can not be easily extended to the case of non uniform magnetic field.

Finally, we study the convergence rate of the Vlasov-Poisson equation (1.1)-(1.3) to the asymptotic model when $\varepsilon \to 0$. We proceed as in the linear case to plot in Figure 11 the convergence of the model (1.1) towards the limit regime. Here again, the rate is close to one.

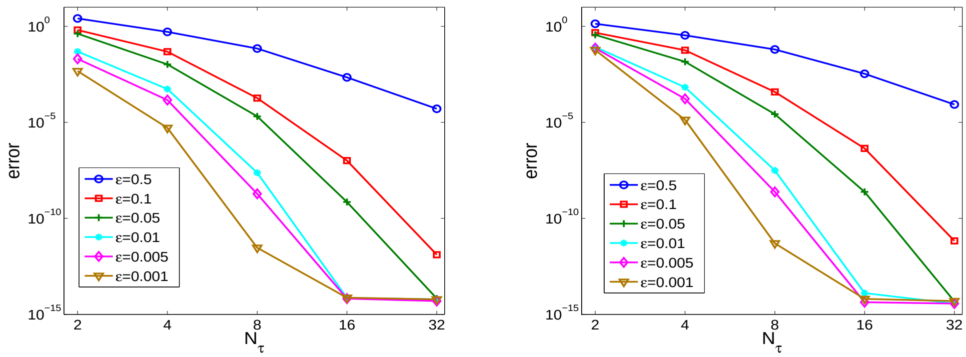

FIGURE 4. Error in τ of IMEX1 with second order initial data (X_k^{2nd}, Y_k^{1st}) for given E case: relative maximum error in ρ^ε (left) and in $\rho^\varepsilon_{\mathbf{v}}$ (right) with respect to the number of grid points N_τ.

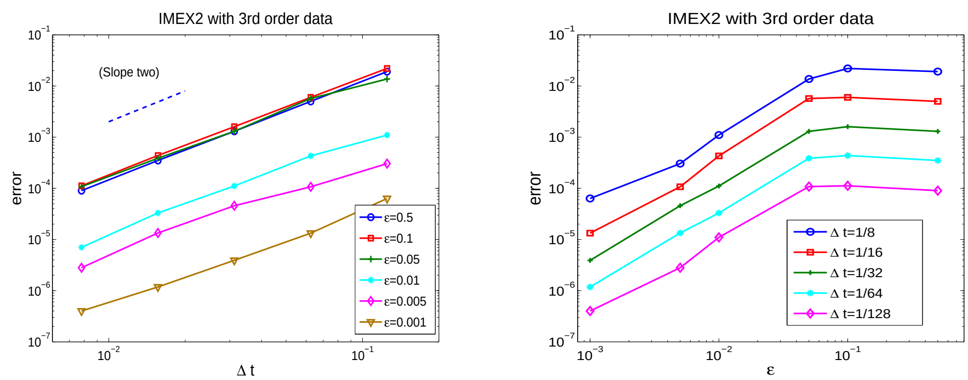

FIGURE 5. Temporal error of IMEX2 with third order initial data (X_k^{3rd}, Y_k^{2nd}) for given E case: relative maximum error in ρ^ε.

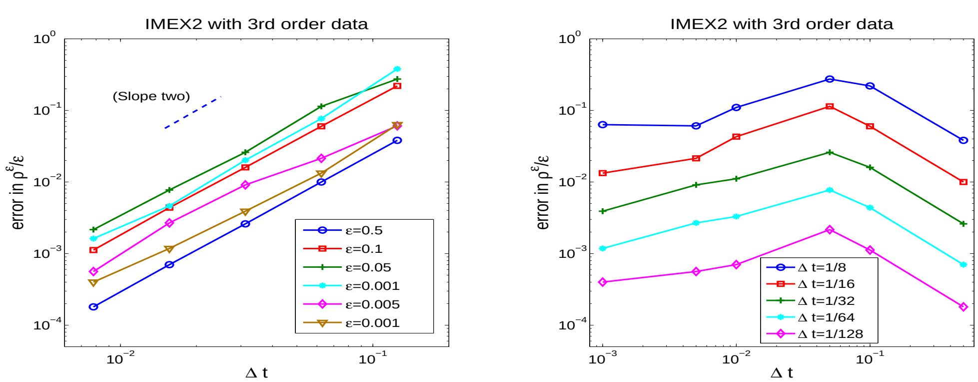

FIGURE 6. Temporal error of IMEX2 with third order initial data (X_k^{3rd}, Y_k^{2nd}) for given E case: relative maximum error in $\rho^\varepsilon/\varepsilon$.

5. CONCLUSION

We proposed a multi-scale numerical scheme for the Vlasov equation with a strong non-homogeneous magnetic field by using a Particle-in-Cell strategy. The solution of the problem is highly oscillatory

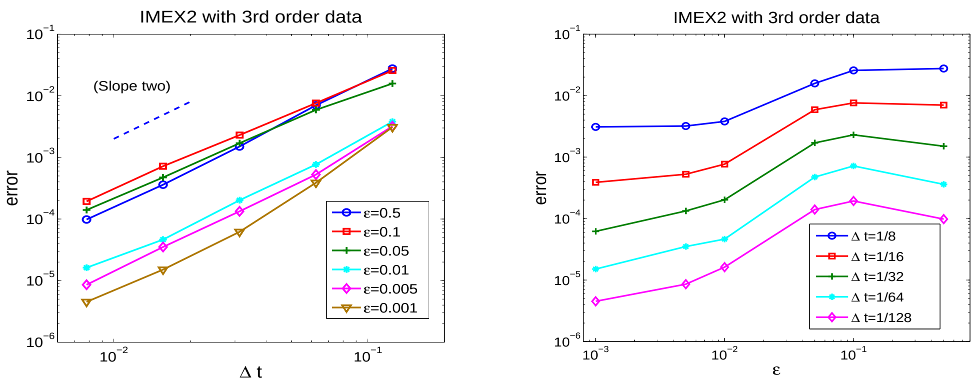

FIGURE 7. Temporal error of IMEX2 with third order initial data (X_k^{3rd}, Y_k^{2nd}) for given E case: relative maximum error in $\rho_{\mathbf{v}}^{\varepsilon}$.

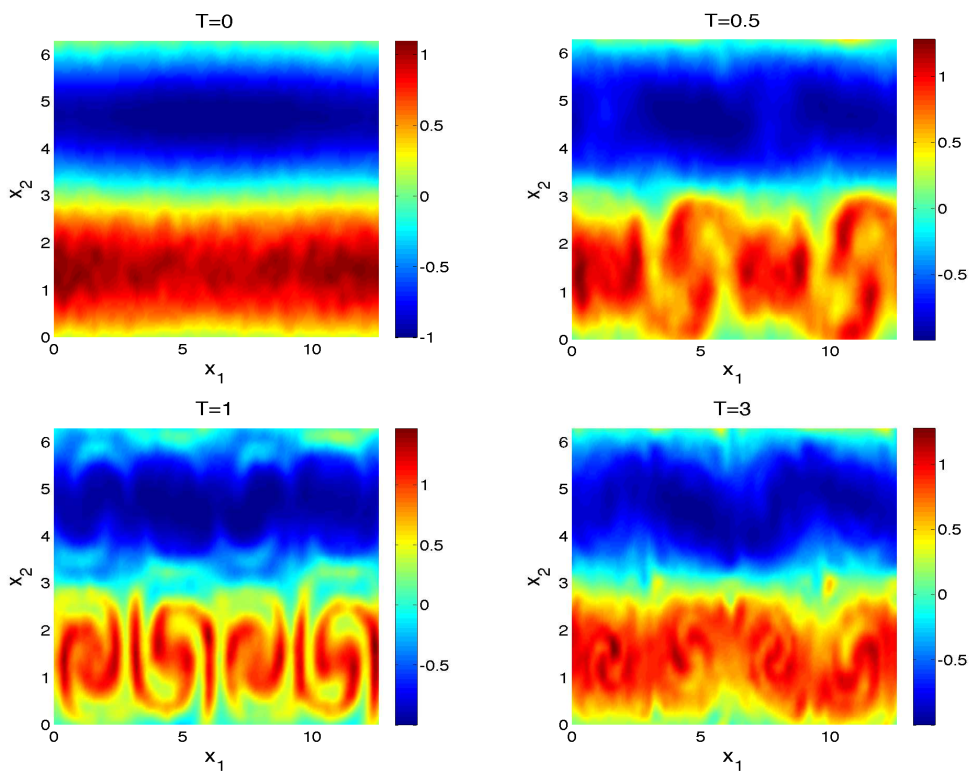

FIGURE 8. 2D plot of $\rho^{\varepsilon}(t, \mathbf{x})$ at different t for given E case with $\varepsilon = 0.1$.

in time, space and velocity with non-periodic oscillation. Making use of the fact that the positions of the particles in this regime are confined around the initial position, we transformed the characteristics into a suitable form which enabled us to perform the separation of scales techniques. A uniformly accurate first order scheme was then proposed and rigorously analyzed for the Vlasov equation with external electric field; for this scheme, we also proved that it enjoys the confinement property at the discrete level. Practical extensions are performed to achieve the second order accuracy, and also to deal with the case of the Vlasov-Poisson equation. In the later case, it turns out that the characteristics equations are a huge highly oscillatory system with multiple frequencies.

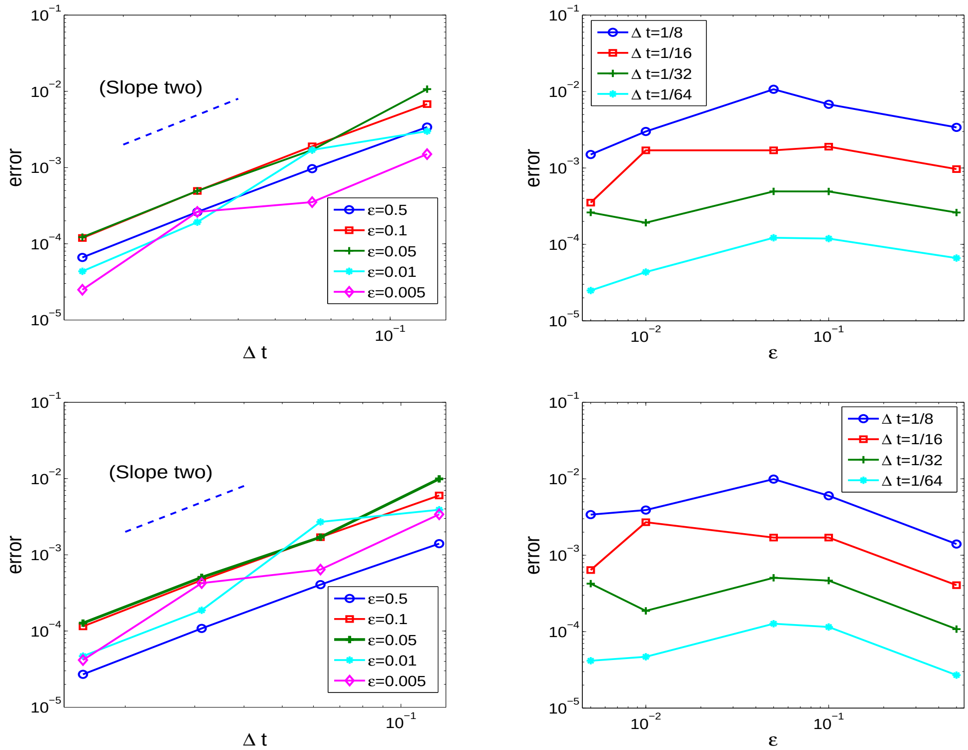

FIGURE 9. Temporal error of EI2 with (X_k^{1st}, Y_k^{1st}) for Vlasov-Poisson case: relative maximum error in ρ^ε (first row) and $\rho^\varepsilon_{\mathbf{v}}$ (second row).

Numerical results are then presented to confirm the theoretical results and illustrate the efficiency of the proposed schemes.

Appendix A. Third order preparation

In this appendix, we derive the third order initial data, which will ensure (following the same strategy used in Proposition 2.1) that the quantities $\frac{1}{\varepsilon}\partial_s^3 X$ and $\partial_s^3 Y$ are uniformly bounded.

We first derive (2.28a) with respect to s and assuming $\partial_s^3 \mathbf{h} = O(\varepsilon)$, we find

$$\partial_s^2 \mathbf{h}(0,\tau) = \tilde{\tilde{\mathbf{h}}}^{1st}(\tau) + O(\varepsilon^2) \quad \text{with } \tilde{\tilde{\mathbf{h}}}^{1st}(\tau) := \frac{\varepsilon}{b^0} A e^{\tau J} \underline{\tilde{\tilde{Y}}}^{0th},$$

where we used the following notations

$$\underline{\tilde{\tilde{Y}}}^{0th} := \frac{\nabla_{\mathbf{x}} b(\mathbf{x}_0)\cdot \underline{\tilde{X}}^{1st}}{\varepsilon b^0} J\mathbf{v}_0 + \frac{1}{\varepsilon}\Pi\left(\frac{b(X^{1st})}{b^0}-1\right) J \underline{\tilde{Y}}^{0th},$$

$$\underline{\tilde{X}}^{1st} := \frac{1}{b^0}\Pi(e^{\tau J}\mathbf{r}^{1st}), \quad \underline{\tilde{Y}}^{0th} := \Pi\frac{1}{\varepsilon}\left(\frac{b(X^{1st})}{b^0}-1\right) J\mathbf{v}_0,$$

with X^{1st} and $\mathbf{r}^{1st}$ given by (2.31) and (2.32). Note that $\partial_s^2 \underline{Y}(0) = \underline{\tilde{\tilde{Y}}}^{0th} + O(\varepsilon)$, $\partial_s \underline{X}(0) = \underline{\tilde{X}}^{1st} + O(\varepsilon^2)$ and $\partial_s \underline{Y}(0) = \underline{\tilde{Y}}^{0th} + O(\varepsilon)$. Similarly, deriving (2.28b) with respect to s and assuming

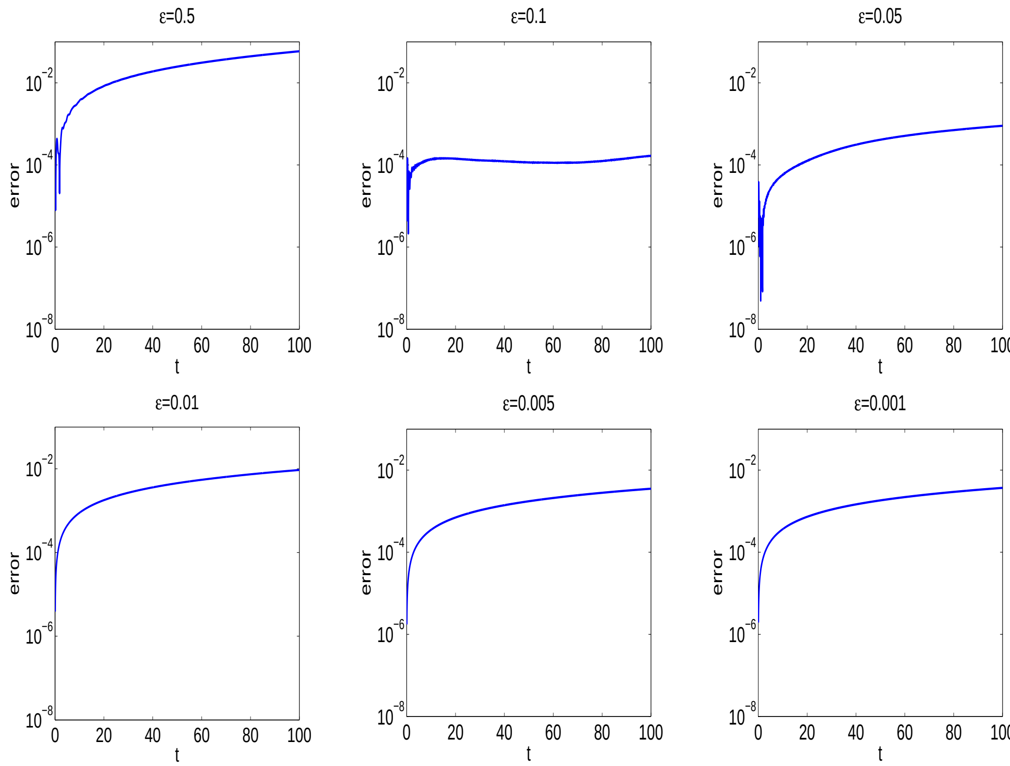

FIGURE 10. Relative energy error $|H(t) - H(0)|/H(0)$ of the EI2 scheme with $\Delta t = 0.05$ for the Vlasov-Poisson case under serval ε.

$\partial_s^3 \mathbf{r} = O(\varepsilon)$, we have

$$\partial_s^2 \mathbf{r}(0,\tau) = \tilde{\tilde{\mathbf{r}}}^{1st}(\tau) + O(\varepsilon^2), \quad \text{with}$$
$$\tilde{\tilde{\mathbf{r}}}^{1st}(\tau) := \frac{2}{b^0} A \nabla_{\mathbf{x}} b(\mathbf{x}_0) \cdot \left(\underline{\tilde{X}}^{1st} + \tilde{\mathbf{h}}^{1st} \right) J \underline{\tilde{Y}}^{0th} + A \left(\frac{b(X^{1st})}{b^0} - 1 \right) J \underline{\tilde{\tilde{Y}}}^{0th}$$
$$+ \frac{1}{b^0} A \nabla_{\mathbf{x}} b(\mathbf{x}_0) \cdot \left(\underline{\tilde{\tilde{X}}}^{1st} + \tilde{\tilde{\mathbf{h}}}^{1st} \right) J \mathbf{v}_0,$$

where we defined

$$\underline{\tilde{\mathbf{h}}}^{1st}(\tau) := \frac{\varepsilon}{b^0} A e^{\tau J} \underline{\tilde{Y}}^{0th}, \qquad \underline{\tilde{\tilde{X}}}^{1st} := \frac{1}{b^0} \Pi e^{\tau J} \tilde{\mathbf{r}}^{1st},$$
$$\tilde{\mathbf{r}}^{1st} := A \left(\frac{b(X^{1st})}{b^0} - 1 \right) J \underline{\tilde{Y}}^{0th} + \frac{1}{b^0} A \nabla_{\mathbf{x}} b(\mathbf{x}_0) \cdot \tilde{\mathbf{h}}^{1st} J \mathbf{v}_0 + \frac{\varepsilon}{(b^0)^2} A e^{-\tau J} \partial_t \mathbf{E}^\varepsilon(0, \mathbf{x}_0).$$

Note that $\underline{\ddot{X}}(0) = \underline{\tilde{\tilde{X}}}^{1st} + O(\varepsilon^2)$. Then we update to get

$$\underline{\tilde{Y}}_k^{1st} = \Pi \left[\frac{1}{\varepsilon} \left(\frac{b(X^{2nd})}{b^0} - 1 \right) J Y^{1st} + e^{-J\tau} \frac{\mathbf{E}^\varepsilon(0, X^{1st})}{b^0} \right],$$
$$\underline{\tilde{X}}^{2nd} = \frac{1}{b^0} \Pi (e^{\tau J} \mathbf{r}^{2nd}),$$

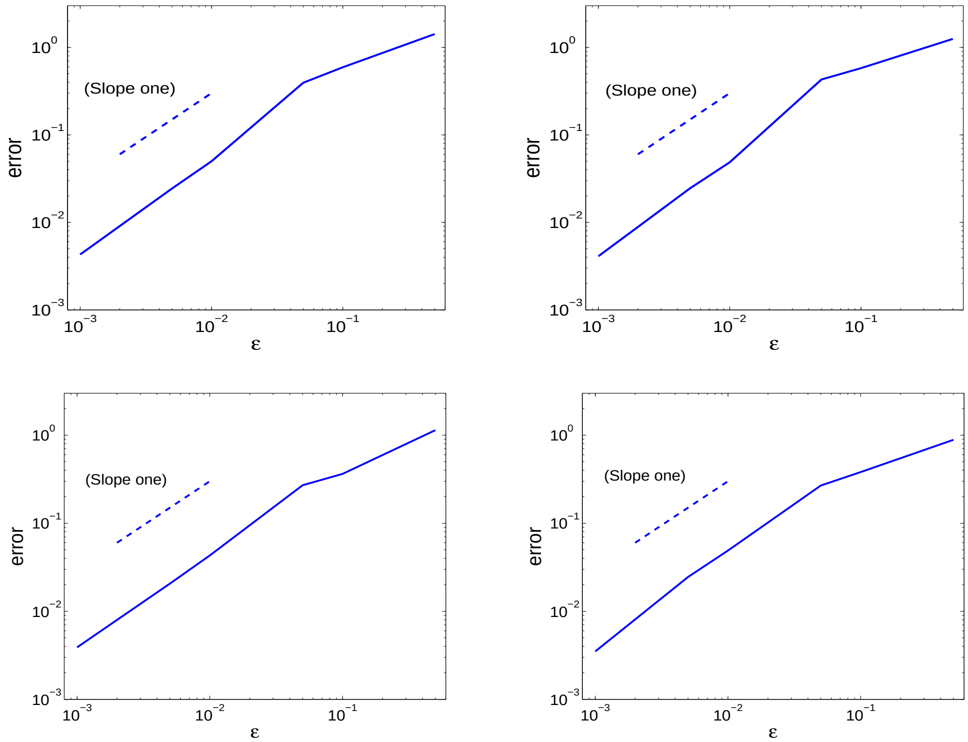

FIGURE 11. Convergence the Vlasov equation (1.1) in the given E case (left) and in the Vlasov-Poisson case (right) to in the limit regime: relative maximum error in ρ^ε (first row) and $\rho^\varepsilon_{\mathbf{v}}$ (second row) at $t_f = 1$.

where X^{2nd} is given by (2.38) and $\mathbf{r}^{2nd}$ by (2.41). Moreover, we define

$$\begin{aligned}
\tilde{\mathbf{h}}^{2nd}(\tau) :=& \frac{\varepsilon}{b^0} A e^{\tau J}\left(\underline{\tilde{Y}}^{1st} + \tilde{\mathbf{r}}^{1st}\right) - \varepsilon L^{-1}\tilde{\tilde{\mathbf{h}}}^{1st},\\
\tilde{\mathbf{r}}^{2nd}(\tau) :=& A\left(\frac{b(X^{2nd})}{b^0} - 1\right) J\left(\underline{\tilde{Y}}^{1st} + \tilde{\mathbf{r}}^{1st}\right)\\
&+ \frac{1}{b^0} A \nabla_{\mathbf{x}} b(X^{1st}) \cdot \left(\underline{\tilde{X}}^{2nd} + \tilde{\mathbf{h}}^{2nd}\right) J Y^{1st}\\
&+ \frac{\varepsilon}{b^0} A e^{-J\tau}\left(\frac{\partial_t \mathbf{E}^\varepsilon(0, X^{1st})}{b^0} + \nabla_{\mathbf{x}}\mathbf{E}^\varepsilon(0, X^{1st})(\underline{\tilde{X}}^{1st} + \tilde{\mathbf{h}}^{1st})\right)\\
&- \varepsilon L^{-1}\tilde{\tilde{\mathbf{r}}}^{1st}.
\end{aligned}$$

Note that $\partial_s \underline{X}(0) = \underline{\tilde{X}}^{2nd} + O(\varepsilon^3)$, $\partial_s \mathbf{h}(0,\tau) = \tilde{\mathbf{h}}^{2nd}(\tau) + O(\varepsilon^3)$ and $\partial_s \underline{Y}(0) = \underline{\tilde{Y}}^{1st} + O(\varepsilon^2)$, $\partial_s \mathbf{r}(0,\tau) = \tilde{\mathbf{r}}^{2nd}(\tau) + O(\varepsilon^3)$.

Eventually from (2.27a), we define iteratively

$$\mathbf{h}^{3rd}(\tau) := \frac{\varepsilon}{b^0} A e^{\tau J} Y^{2nd} - \varepsilon L^{-1}\tilde{\mathbf{h}}^{2nd},$$

where Y^{2nd} is given by (2.43), so that the third order initial data for the first equation is

$$X^{3rd}(\tau) := \mathbf{x}_0 + \mathbf{h}^{3rd}(\tau) - \mathbf{h}^{3rd}(0). \tag{A.1}$$

We can than define

$$\mathbf{r}^{3rd}(\tau) := A\left(\frac{b(X^{3rd})}{b^0} - 1\right) e^{\tau J} Y^{2nd} + \frac{\varepsilon}{b^0} A e^{-J\tau}\mathbf{E}^\varepsilon(0, X^{2nd}) - \varepsilon L^{-1}\tilde{\mathbf{r}}^{2nd},$$

so that the third order initial data for the second equation is

$$Y^{3rd}(\tau) := \mathbf{v}_0 + \mathbf{r}^{3rd}(\tau) - \mathbf{r}^{3rd}(0). \tag{A.2}$$

Note that $\mathbf{h}(0,\tau) = \mathbf{h}^{3rd}(\tau) + O(\varepsilon^4)$ and $\mathbf{r}(0,\tau) = \mathbf{r}^{3rd}(\tau) + O(\varepsilon^4)$.

Proposition A.1. *Assume (2.4) and $E^\varepsilon(t,\mathbf{x}) \in \mathcal{C}^4([0,T]\times\mathbb{R}^2)$ and $b(\mathbf{x}) \in \mathcal{C}^4(\mathbb{R}^2)$. With the third order initial data $X(0,\tau) = X^{3rd}(\tau)$ given by* (A.1) *and $Y(0,\tau) = Y^{2nd}(\tau)$ given by* (2.43)*, the solution of the two-scale system (2.13) satisfies*

$$\frac{1}{\varepsilon}\|\partial_s^\ell X\|_{L_s^\infty(W_\tau^{1,\infty})} + \|\partial_s^\ell Y\|_{L_s^\infty(W_\tau^{1,\infty})} \le C_0, \quad \ell = 1,2,3,$$

for some constant $C_0 > 0$ independent of ε.

Proof. The proof is a recursive process of the known results and it is very similar to that of Proposition 2.1. We omit the details here for brevity. □

Appendix B. Limit model

In this appendix, we derive limit mode at the characteristics level. From (2.25)-(2.26), we derive the averaged model by considering $\varepsilon \ll 1$. Indeed, from the equations on $\mathbf{h}$ and $\mathbf{r}$, we get

$$\begin{aligned}
\mathbf{h} &= -\frac{\varepsilon}{b^0} J\mathrm{e}^{\tau J}\underline{Y} + O(\varepsilon^2),\\
\mathbf{r} &= -\frac{\varepsilon}{(b^0)^2}\mathrm{e}^{\tau J}\underline{Y}\cdot\nabla_{\mathbf{x}} b(\underline{X}) J\underline{Y} + \frac{\varepsilon}{b^0} J\mathrm{e}^{-\tau J}\mathbf{E}^\varepsilon(s/b^0,\underline{X}) + O(\varepsilon^2).
\end{aligned}$$

Then, injecting in the macro equations on $\underline{X}$ and $\underline{Y}$, we obtain

$$\begin{aligned}
\partial_s\underline{X} &= -\frac{\varepsilon}{(b^0)^3}\Pi\left[\mathrm{e}^{\tau J}(\mathrm{e}^{\tau J}\underline{Y}\cdot\nabla_{\mathbf{x}} b(\underline{X}))J\underline{Y}\right] + \frac{\varepsilon}{(b^0)^2}\Pi\left[\mathrm{e}^{\tau J}J\mathrm{e}^{-\tau J}\mathbf{E}^\varepsilon(s/b^0,\underline{X})\right] + O(\varepsilon^2),\\
\partial_s\underline{Y} &= \frac{1}{\varepsilon}\Pi\left[B(\underline{X}+\mathbf{h})J\underline{Y}\right] + \Pi\left[\mathrm{e}^{-\tau J}\frac{1}{b^0}\mathbf{E}^\varepsilon(s/b^0,\underline{X})\right] + O(\varepsilon),
\end{aligned}$$

where we defined $B(X) = b(X)/b(\mathbf{x}_0) - 1$. After some computations, it comes

$$\begin{aligned}
\partial_s\underline{X} &= -\frac{\varepsilon}{2(b^0)^3}J\nabla_{\mathbf{x}} b(\underline{X})\,|\underline{Y}|^2 + \frac{\varepsilon}{(b^0)^2}J\mathbf{E}^\varepsilon(s/b^0,\underline{X}) + O(\varepsilon^2),\\
\partial_s\underline{Y} &= \frac{1}{\varepsilon}B(\underline{X})J\underline{Y} + O(\varepsilon),\\
&= \frac{1}{\varepsilon b^0}(b(\underline{X}) - b^0)J\underline{Y} + O(\varepsilon).
\end{aligned}$$

Under the fact that $b(\mathbf{x}(t)) = b^0 + O(\varepsilon)$, the limit model above is consistent with the one derived in [16, 3].

Acknowledgements

This work is supported by the French ANR project MOONRISE ANR-14-CE23-0007-01. N. Crouseilles and M. Lemou are supported by the Enabling Research EUROFusion project CfP-WP14-ER-01/IPP-03. X. Zhao is supported by the IPL FRATRES. This work has been carried out within the framework of the French Federation for Magnetic Fusion Studies (FR-FCM) and of the Eurofusion consortium, and has received funding from the Euratom research and training programme 2014-2018 and 2019-2020 under grant agreement No 633053. The views and opinions expressed herein do not necessarily reflect those of the European Commission.

References

[1] C.K. Birdsall, A.B. Langdon, Plasma Physics via Computer Simulation, Adam Hilger, 1991.

[2] M. Bostan, The Vlasov-Maxwell system with strong initial magnetic field. Guiding-center approximation, SIAM J. Multiscale Model. Simul. 6 (2007), pp.1026-1058.

[3] M. Bostan, Asymptotic behavior for the Vlasov-Poisson equations with strong external magnetic field. Straight magnetic field lines. preprint (2018), hal-01683869.

[4] M. Bostan, A. Finot, The effective Vlasov-Poisson system for the finite Larmor radius regime, SIAM J. Multiscale Model. Simul. 14 (2015), pp. 1238-1275.

[5] M.P. Calvo, Ph. Chartier, A. Murua, J.M. Sanz-Serna, Numerical experiments with the stroboscopic method, Appl. Numer. Math. 61 (2011), pp. 1077-1095.

[6] M.P. Calvo, Ph. Chartier, A. Murua, J.M. Sanz-Serna, A stroboscopic numerical method for highly oscillatory problems, in Numerical Analysis and Multiscale Computations, B. Engquist, O. Runborg and R. Tsai, editors, Lect. Notes Comput. Sci. Eng., Vol. 82, Springer 2011, 73-87.

[7] Ph. Chartier, N. Crouseilles, M. Lemou, An averaging technique for transport equations, arXiv:1609.09819v1, submitted, 2016.

[8] Ph. Chartier, N. Crouseilles, M. Lemou, F. Méhats, Uniformly accurate numerical schemes for highly oscillatory Klein-Gordon and nonlinear Schrödinger equations, Numer. Math. 129 (2015), pp. 211-250.

[9] P. Chartier, M. Lemou, F. Méhats, Highly-oscillatory evolution equations with non-resonant frequencies: averaging and numerics, Numer. Math. 136 (2017), pp. 907-939.

[10] Ph. Chartier, M. Lemou, F. Méhats, G. Vilmart, A new class of uniformly accurate methods for highly oscillatory evolution equations, hal-01666472, 2017.

[11] Ph. Chartier, J. Makazaga, A. Murua, G. Vilmart, Multi-revolution composition methods for highly oscillatory differential equations, Numer. Math. 128 (2014), pp 167-192.

[12] Ph. Chartier, N. Mauser, F. Méhats, Y. Zhang, (Solving highly-oscillatory NLS with SAM: numerical efficiency and geometric properties), DCDS 9 (2016), pp. 1327-1349.

[13] N. Crouseilles, M. Lemou, F. Méhats, Asymptotic preserving schemes for highly oscillatory Vlasov-Poisson equations, J. Comput. Phys. 248 (2013) pp. 287-308.

[14] N. Crouseilles, M. Lemou, F. Méhats, X. Zhao, Uniformly accurate forward semi-Lagrangian methods for highly oscillatory Vlasov-Poisson equations, SIAM Multiscale Model. Simul. 15 (2017), pp. 723-744.

[15] N. Crouseilles, M. Lemou, F. Méhats, X. Zhao, Uniformly accurate Particle-in-Cell method for the long time two-dimensional Vlasov-Poisson equation with uniform strong magnetic field, J. Comput. Phys. 346 (2017), pp. 172-190.

[16] P. Degond, F. Filbet, On the asymptotic limit of the three dimensional Vlasov-Poisson system for large magnetic field: formal derivation, J. Stat. Physicists. 65 (2016), pp. 765-784.

[17] F. Filbet, T. Xiong, E. Sonnendrücker, On the Vlasov-Maxwell system with a strong magnetic field, SIAM J. Applied Mathematics 78 (2018), pp. 1030-1055.

[18] F. Filbet, M. Rodrigues, Asymptotically stable particle-in-cell methods for the Vlasov-Poisson system with a strong external magnetic field, SIAM J. Numer. Analysis 54 (2016), pp. 1120-1146.

[19] F. Filbet, M. Rodrigues, Asymptotically preserving particle-in-cell methods for inhomogeneous strongly magnetized plasmas, SIAM J. Numer. Anal. 55 (2017), pp. 2416-2443.

[20] E. Frénod, F. Salvarani and E. Sonnendrücker, Long time simulation of a beam in a periodic focusing channel via a two-scale PIC-method, Math. Models Methods Appl. Sci. 19 (2009), pp. 175-197.

[21] E. Frénod, E. Sonnendrücker, Long time behavior of the two-dimensional Vlasov equation with a strong external magnetic field, Math. Models Methods Appl. Sci. 10 (2000), pp. 539-553.

[22] E. Frénod, S.A. Hirstoaga, M. Lutz, E. Sonnendrücker, Long time behavior of an exponential integrator for a Vlasov-Poisson system with strong magnetic field, Commun. in Comput. Phys. 18 (2015), pp. 263-296.

[23] G.B. Jacobs, J.S. Hesthaven, Implicit-Explicit time integration of a high-order particle-in-cell method with hyperbolic divergence cleaning, Comput. Phys. Comm. 180 (2009), pp. 1760-1767.

[24] S. Jin, Efficient asymptotic-preserving (AP) schemes for some multiscale kinetic equations, SIAM J. Sci. Comput. 21 (1999), pp. 441-454.

[25] W.W. Lee, Gyrokinetic approach in particle simulation, Phys. Fluids 26 (1983).

[26] L. Saint-Raymond, The gyro-kinetic approximation for the Vlasov-Poisson system, Math. Models Methods Appl. Sci. 10 (2000), pp. 1305-1332.

[27] E. Sonnendrücker, Numerical Methods for Vlasov Equations, Lecture notes, 2016.

Ph. Chartier: Univ Rennes, INRIA-MINGuS, CNRS, IRMAR-UMR 6625, F-35000 Rennes, France
E-mail address: Philippe.Chartier@inria.fr

N. Crouseilles: Univ Rennes, INRIA-MINGuS, CNRS, IRMAR-UMR 6625, F-35000 Rennes, France
E-mail address: nicolas.crouseilles@inria.fr

M. Lemou: Univ Rennes, CNRS, INRIA-MINGuS, IRMAR-UMR 6625, F-35000 Rennes, France
E-mail address: mohammed.lemou@univ-rennes1.fr

F. Méhats: Univ Rennes, INRIA-MINGuS, CNRS, IRMAR-UMR 6625, F-35000 Rennes, France
E-mail address: florian.mehats@univ-rennes1.fr

X. Zhao: Univ Rennes, INRIA-MINGuS, CNRS, IRMAR-UMR 6625, F-35000 Rennes, France
E-mail address: zhxfnus@gmail.com